ARMY RESEARCH LABORATORY

Electrothermal-Chemical (ETC) Propulsion With High Loading Density Charges

Kevin J. White
William F. Oberle
Arpad A. Juhasz
Irvin C. Stobie
MAJ Kevin Nekula
Gary L. Katulka
Simon Driesen

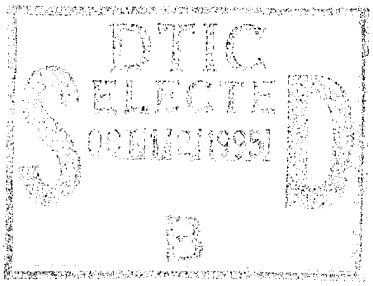

ARL-TR-845 August 1995

NOTICES

Destroy this report when it is no longer needed. DO NOT return it to the originator.

Additional copies of this report may be obtained from the National Technical Information Service, U.S. Department of Commerce, 5285 Port Royal Road, Springfield, VA 22161.

The findings of this report are not to be construed as an official Department of the Army position, unless so designated by other authorized documents.

The use of trade names or manufacturers' names in this report does not constitute indorsement of any commercial product.

REPORT DOCUMENTATION PAGE

Form Approved
OMB No. 0704-0188

1. AGENCY USE ONLY *(Leave blank)*	2. REPORT DATE	3. REPORT TYPE AND DATES COVERED
	August 1995	Final, December 1993-December 1994

4. TITLE AND SUBTITLE

Electrothermal-Chemical Propulsion with High Loading Density Charges

5. FUNDING NUMBERS

PR: 1L162618AH80

6. AUTHOR(S)

Kevin J. White, William F. Oberle, Arpad A. Juhasz, Irvin C. Stobie,
MAJ Kevin Nekula, Gary L. Katulka, and Simon Driesen

7. PERFORMING ORGANIZATION NAME(S) AND ADDRESS(ES)

U.S. Army Research Laboratory
ATTN: AMSRL-WT-PA
Aberdeen Proving Ground, MD 21005-5066

8. PERFORMING ORGANIZATION REPORT NUMBER

ARL-TR-845

9. SPONSORING/MONITORING AGENCY NAMES(S) AND ADDRESS(ES)

10.SPONSORING/MONITORING AGENCY REPORT NUMBER

11. SUPPLEMENTARY NOTES

12a. DISTRIBUTION/AVAILABILITY STATEMENT

Approved for public release; distribution is unlimited.

12b. DISTRIBUTION CODE

13. ABSTRACT *(Maximum 200 words)*

This report investigates and quantifies the requirements for increasing performance (muzzle kinetic energy) in existing high performance (tank) gun systems utilizing solid propellants. Factors studied include propelling charge mass or loading density, propellant specific energy, grain geometry, and the use of electrothermal-chemical concepts.

Results indicate that significant increases in performance require not only increased system energy but, more importantly, propellant combustion control in terms of the mass generation rate to operate near "ideal" gun performance. Specific requirements and approaches (e.g., propellant burn rate modification by plasma radiative heating) to obtain the "ideal" gun performance are discussed. Pertinent experimental results are also included.

14. SUBJECT TERMS

ETC, ballistics, radiation, high loading density, electrothermal chemical, solid propellants

15. NUMBER OF PAGES

43

16. PRICE CODE

17. SECURITY CLASSIFICATION OF REPORT	18. SECURITY CLASSIFICATION OF THIS PAGE	19. SECURITY CLASSIFICATION OF ABSTRACT	20. LIMITATION OF ABSTRACT
UNCLASSIFIED	UNCLASSIFIED	UNCLASSIFIED	UL

INTENTIONALLY LEFT BLANK.

ACKNOWLEDGMENTS

The authors would like to acknowledge Fred Robbins for his insightful discussions and suggestions during the course of this work, Ron Anderson for his help with aspects of the calculations, and Anna Wildegger-Gassmaier and Joe Heimerl for their careful reading and editing of the manuscript.

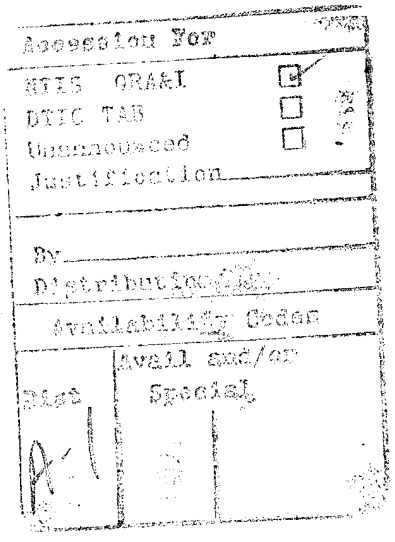

INTENTIONALLY LEFT BLANK.

TABLE OF CONTENTS

INTENTIONALLY LEFT BLANK.

LIST OF FIGURES

INTENTIONALLY LEFT BLANK.

LIST OF TABLES

INTENTIONALLY LEFT BLANK.

1. INTRODUCTION

Gun systems in use within the military can generally increase lethality and/or survivability when operating at higher projectile muzzle velocities. Such higher performance will yield longer ranges for artillery, shorter time-of-flight for antiaircraft guns, and longer standoff or better armor penetration for tank guns. With current budgetary constraints, it is advantageous to look for performance improvement using existing weapons. This retrofitting will necessitate using concepts that must operate within certain constraints imposed by existing systems. For guns, this means operating at or below specified maximum pressures with a predetermined maximum gun chamber volume and a given gun tube length.

The objective of this report is to examine propulsion options such as high loading densities, high-energy propellants, and electrothermal-chemical (ETC) propulsion and to determine performance improvements possible in a 120-mm tank cannon. Although other propellant systems such as liquids and slurries are also being considered to improve performance (Chiu and King 1993; Juhasz et al. 1993), this report is confined to the study of solid propellants.

2. IDEAL GUN PERFORMANCE

We will consider here the optimum performance potential of the M256 120-mm tank cannon. The maximum ideal performance of the gun is achieved when the propellant ignites and generates sufficient gas to immediately reach the maximum operating pressure. As the projectile moves down bore, the propellant mass generation rate is such that a constant pressure (CP) is maintained in the breech until the propellant is consumed. The projectile continues to move down bore to the muzzle exit, driven by an adiabatic isentropic expansion of the gases. This process imparts the theoretical maximum energy for a given amount of propellant to the projectile within the constraints of the gun envelope. Such an idealized pressure-time history is illustrated as (A) in Figure 1. (These calculations were performed with the IBHVG2 [Anderson and Fickie 1987] interior ballistics code.)

In its essential form, the energy of the burning propellant is converted into the kinetic energy of the projectile, the kinetic energy of the accelerating gases, and the residual internal energy of the gases in the gun. Some energy is also lost to heating the gun walls, recoil, rotating projectile, etc., but the sum of these contributions is negligible compared to the first three. Figure 1 illustrates the calculated pressure-time histories for a 19-perforation propellant (B) where the mass of propellant (input energy) is the same

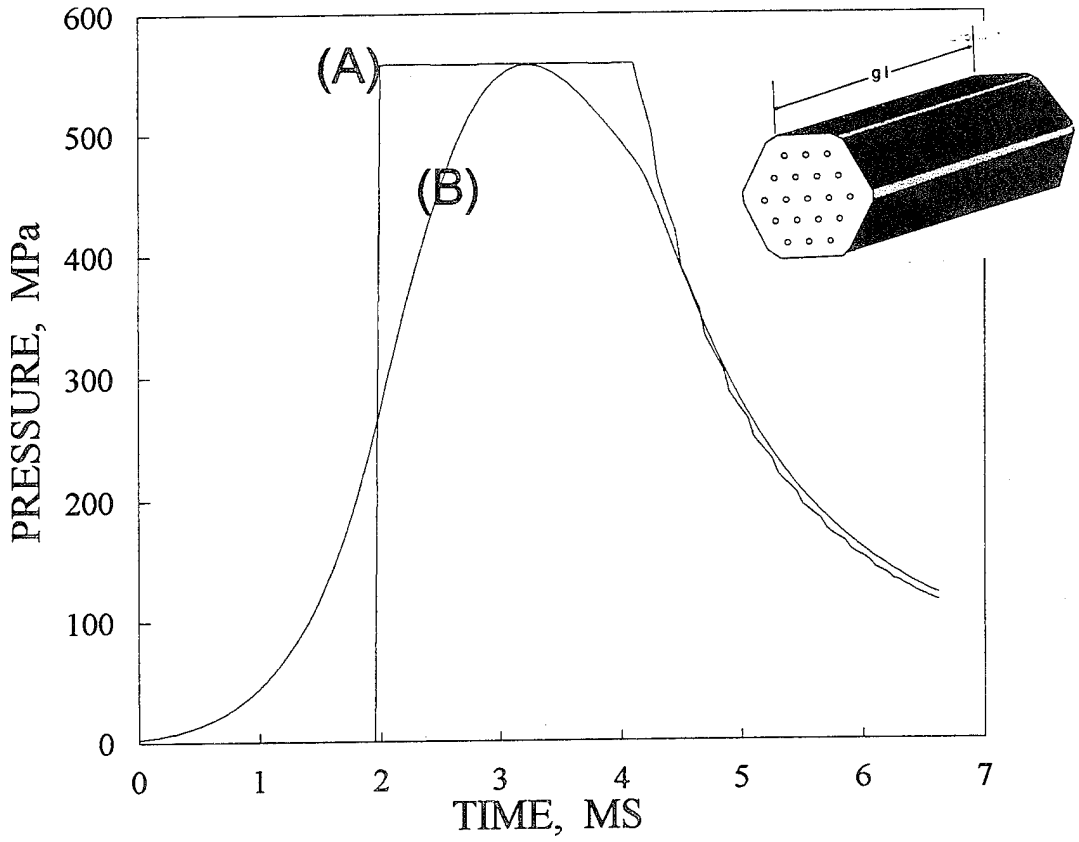

Figure 1. Pressure history calculations; (A) constant pressure, (B) 19-perf.

as utilized in the CP calculation (A). A representative "19-perf" hexagonal grain is illustrated in Figure 1. The "web" is defined as the distance between the perforations.

Table 1 gives a listing of several different caliber guns and experimental velocities along with corresponding results from constant pressure calculations (no losses were assumed). It is clear from Table 1 that existing guns have been designed to perform in a nearly ideal fashion for a given mass of propellant—that is, the experimental velocities are within 90–95% of this ideal velocity. Thus, if significant performance improvement is to be realized, a substantial increase in energy input to the gun, combined with continued nearly ideal operation, must be obtained. Increasing the energy in the chamber can be achieved by (a) increasing the mass of propellant or loading density (LD) (which is the mass of propellant/chamber volume), (b) increasing the inherent chemical energy of the propellant, or (c) introducing electrical energy in the form of a plasma. These concepts and their implementation (i.e., attempting to operate at ideal conditions in a 120-mm cannon) are discussed in the following sections.

Table 1. Experimental and Constant Pressure Velocities for Various Cannons

Gun	Caliber (mm)	Vel. Exp. (m/s)	Vel. CP (m/s)	V_{exp}/V_{CP}
L70	40	1,005	1,079	0.93
IMI	60	1,620	1,781	0.91
M68	105	1,486	1,620	0.92
XM25	120	1,739	1,828	0.95
5"/54	127	839	879	0.95
M198	155	826	884	0.93

3. PERFORMANCE CALCULATIONS

3.1 Increased Propellant Mass or Loading Density. Interior ballistic calculations were carried out to determine the performance improvement by increasing the propellant mass or LD. The performance change is measured in percent change in projectile energy (1/2 mv^2) at the muzzle compared with the M829A1 cartridge used in the M256 120-mm tank cannon. The pressure-time history for this cartridge is shown as (B) in Figure 1. Figure 2 summarizes these calculations for several propellant grain geometries (1- and 7-perforation cylindrical and 19- and 37-perforation hexagonal). The x-axis represents the percent increase in total chemical energy obtained by increasing charge mass (i.e., loading density relative to the baseline M829A1, which is 0.9 g/cm^3). The origin of this graph or zero point baseline represents the reference muzzle energy of the M829A1 cartridge. The calculations were carried out in the following way: for a given loading density, the perforation diameter was fixed at a nominal practical value (0.558 mm); a nominal grain length was chosen; and the web (and consequently the grain diameter) was allowed to vary to achieve the prespecified maximum pressure of 558 MPa. These calculations then give the maximum velocity consistent with the gun and propellant constraints. The muzzle energy change for this calculation was then plotted in Figure 2. Results are given for loading density increases of 20, 40, and 50%. The constant pressure calculation that represents the best possible performance is also shown. It is disappointing to note that not only is the increase in performance with increasing loading density small (for the granulations shown), but in most cases it actually decreases.

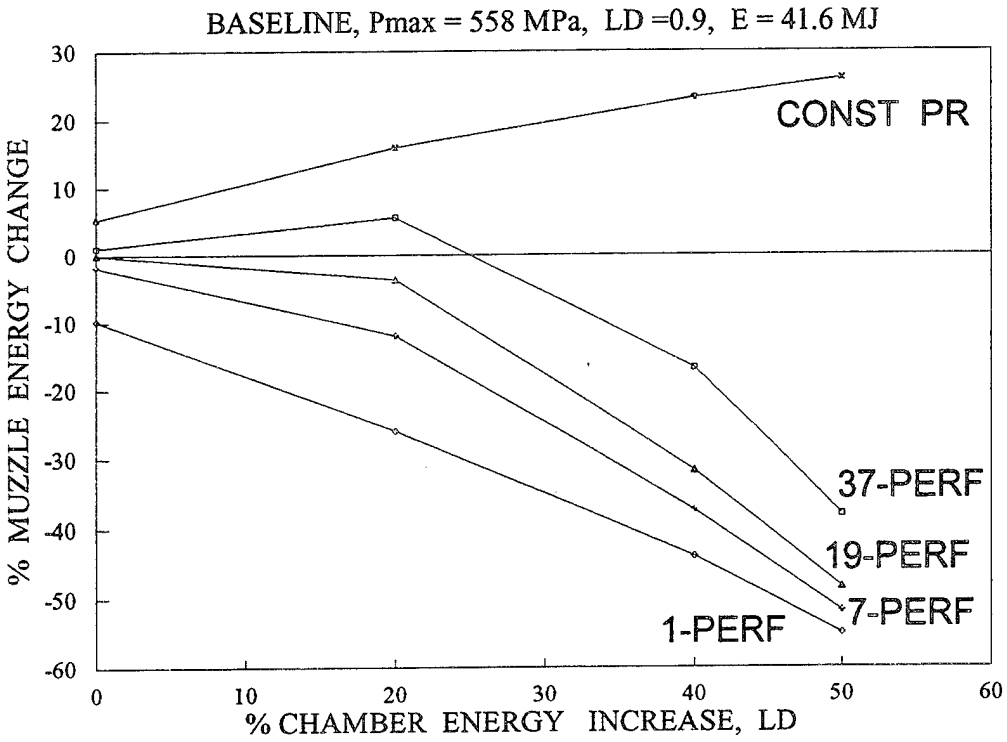

Figure 2. Potential performance change with increased LD.

What is the reason for these results? The primary reason lies in the maximum pressure constraint of 558 MPa and its implications on the mass generation rate, dm/dt, of the propellant. Simplified versions of the equations describing the pressurization process within the gun chamber are given in equations 1–3.

$$PV = (RT/W) \times m \,, \tag{1}$$

$$dm/dt = \rho \times S \times r \,, \tag{2}$$

and

$$r = b \times P^{n} \,, \tag{3}$$

where

P = chamber pressure,

V = free volume in the chamber,

R = gas constant,

T = propellant gas temperature,

W = molecular weight of propellant gas,

m = mass of propellant,

ρ = solid propellant density,

S = solid propellant total surface area,

r = propellant linear burn rate, and

b,n = propellant specific parameters.

If the propellant loading density is increased, then the free volume, V, in the chamber is decreased. Thus, for increased loading density, to keep the pressure P in equation 1 from exceeding the maximum allowed, the mass of propellant m at a given time (found from equation 2) must be decreased (T and W for solid propellant products remain essentially constant at maximum pressure). Since ρ and r for a given propellant at pressure P are fixed, the surface area, S, must be decreased. In practice this is accomplished by changing the dimensions of the grain such as that shown in Figure 1, specifically by increasing the web. However, calculations have shown that the burning surface area *after* the maximum pressure has been reached is also smaller than for the lower LD case. Consequently, the propellant may not burn out before the projectile reaches the muzzle. This is illustrated in Table 2. As an example, at a 40% increase in LD, only 58% of the 19-perf propellant is consumed before the projectile exits the gun. In Figure 3, a calculation of the pressure-time histories for this condition (B) and the constant pressure condition (A) is given.

Table 2. Propellant Mass Fraction (Z) Burned at Muzzle Exit for LD Increase

LD Increase (%)	37-Perf (Z)	19-Perf (Z)	7-Perf (Z)	1-Perf (Z)
0	1.00	1.00	1.00	1.00
20	1.00	0.98	0.90	0.69
40	0.79	0.58	0.50	0.42
50	0.51	0.38	0.34	0.31

After the maximum pressure, there is a much steeper pressure drop than for the situation depicted in Figure 1. The total propellant surface area for this case does not allow all the propellant to burn before

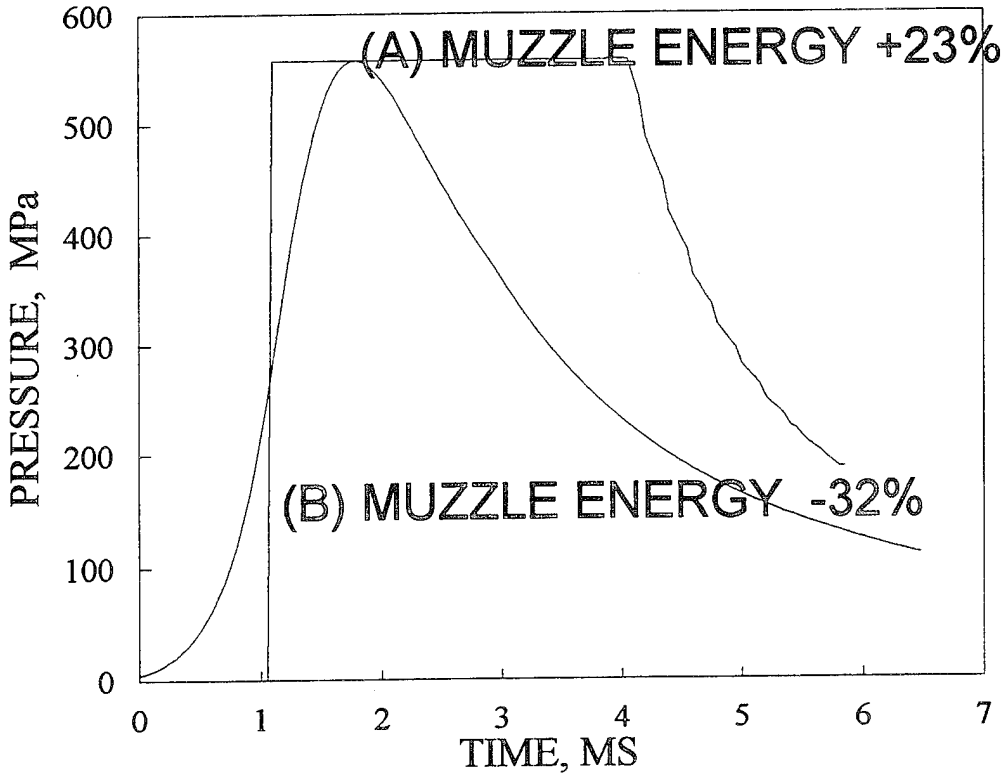

Figure 3. Pressure-time history calculations for 40% increase in LD for (A) constant pressure and (B) 19-perf hex.

muzzle exit. Examination of Figure 2 shows that for a 40% increase in LD, the constant pressure calculation yields a 23% *increase* in muzzle energy, but the 19-perf propellant shows a 32% *decrease* compared with the baseline case. To illustrate this quantitatively, calculations were carried out for the baseline (19-perf) case, with a charge whose increase in loading density was +50%. The resultant pressure-time and propellant total surface area-time data are plotted in Figure 4.

It is seen that the initial surface area for the entire charge at time t = 0, for the baseline calculation is 3.2 m^2, and for the +50% LD is 2 m^2. Just beyond the maximum pressure the baseline surface area is 5 m^2 whereas that of the +50% LD case is 2.5 m^2. Note also that pressure-time curve for the baseline case is much broader than for the +50% case. Figure 5 shows the surface area for the 19-perf grain as a function of time for a number of cases, starting with the baseline case and going to an increase in LD of 20%. A systematic decrease in surface area can be observed throughout the ballistic cycle as the loading density increases.

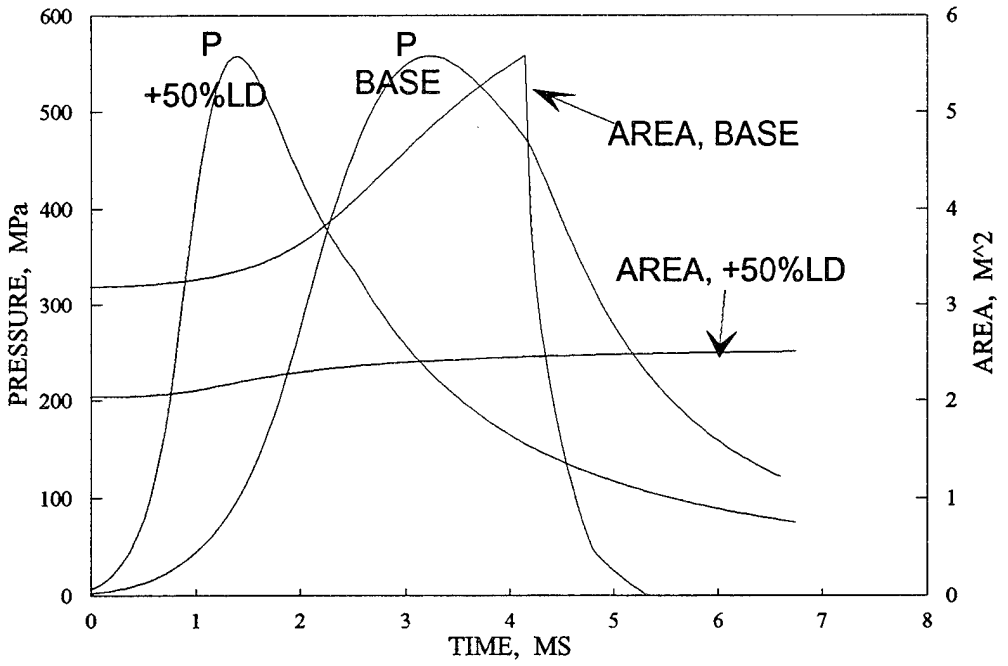

Figure 4. Pressure and area vs. time for baseline and +50% LD.

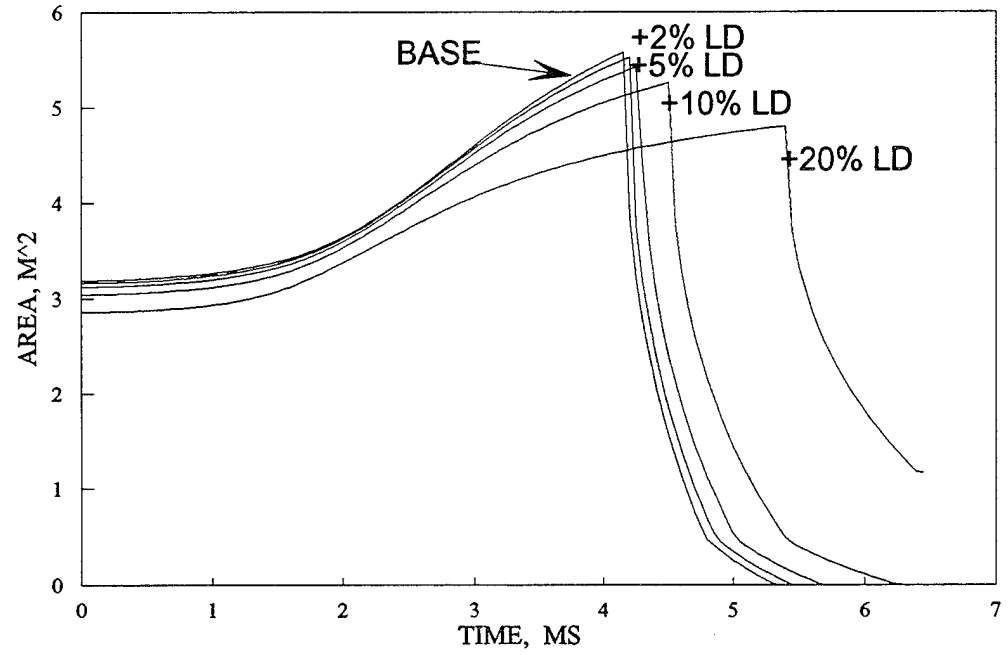

Figure 5. Total surface area vs. time; baseline, +2%, +5%, +10%, +20% LD.

Referring to Figure 2, the charges incorporating 37-perf grains geometry performed better than the 19-perf because of the fact that the surface area for this geometry is more progressive—that is, the surface area increases more rapidly as the propellant burns, increasing the mass generation rate later in time as seen in Figure 6 (19-perf [C]; 37-perf [D]). The surface area increase is smaller for the 7-perf grain (B) as is seen in Figure 6. In the case of the 1-perf geometry (A), the surface area actually decreases as the propellant burns, resulting in a smaller amount of propellant burned prior to muzzle exit and consequently a lower velocity.

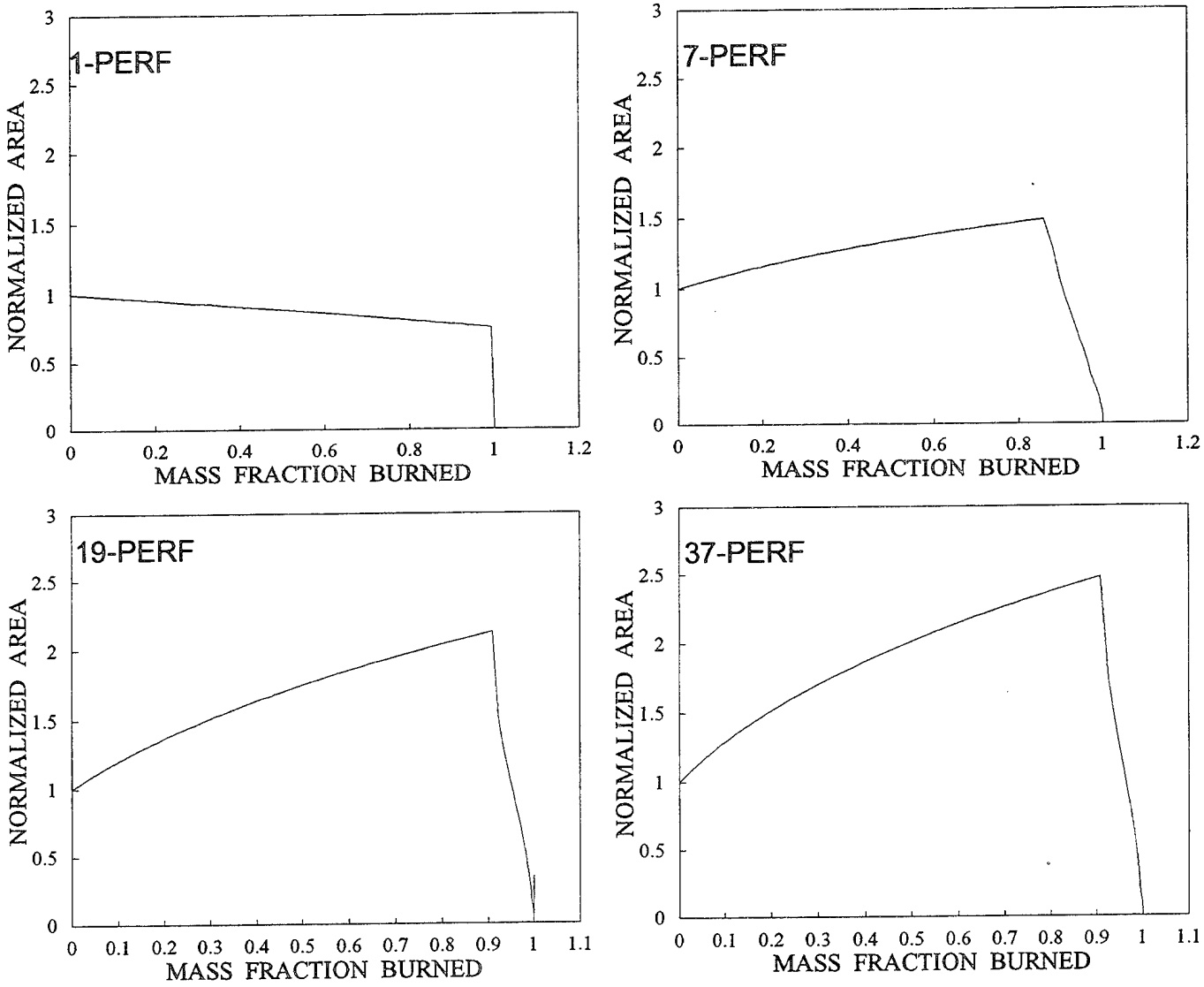

Figure 6. Normalized area vs. mass fraction burned; (A) 1-perf, (B) 7-perf, (C) 19-perf, (D) 37-perf.

Nominal practical perf diameters and length/diameter ratios were chosen for these calculations. The normalized surface area is defined as the total surface area after a given mass fraction has burned divided by the total surface area of the unburned propellant. The surface area for a 1-perf geometry actually decreases as the propellant burns. The 37-perf shows the largest increase. Table 2 lists the mass fraction of the propellant burned at muzzle exit for all of the grain geometries illustrated in Figure 2.

To summarize, although increasing loading density will provide additional energy, current solid propellant geometries (assuming no change in propellant burn rate) will not permit operation near the constant pressure profile (Figure 2). Consequently, the potential performance gain from the increased loading density cannot be realized without burn rate modification, as discussed later in this report.

3.2 Increasing Propellant Energy or Adding Electrical Energy. Calculations were carried out to examine the percent muzzle energy change when increasing the thermochemical energy density (impetus increase without a change in γ) of the propellant or by introducing electrical energy without changing propellant mass. The way the latter is accomplished will be discussed in a subsequent section, but for now it will be treated the same way as an increase in chemical energy—that is to say, the propellant chemical energy will be increased numerically by the amount of electrical energy added (this assumes a 100% efficiency of electrical energy to chemical energy conversion).

As described in the previous section, calculations optimized with respect to velocity were carried out with a fixed perf diameter and a fixed grain length. The web was varied to achieve the 558 MPa. Figure 7 shows the results. The 7-, 19-, and 37-perf grain propellants show performance improvement, but the 1-perf does not. Referring again to equation 1, the mass of the propellant and, hence, the free volume in the chamber has not changed. However, the energy has increased. The energy is directly proportional to the temperature T, and (for fixed molecular weight, W) consequently the mass m(t) must be decreased, just as in the increased loading density case, so as not to exceed the maximum operating pressure. As previously discussed, this must be accomplished by decreasing the surface area, S, which leads to a surface area inadequate for complete combustion of the propellant for most grain geometries. Table 3 shows the mass fraction burned at muzzle exit for all grain geometries shown in Figure 7. However, as opposed to the LD increase in Figure 2, there are substantial increases in performance compared to the zeropoint chamber energy for each grain geometry, although, in the 1-perf case, the performance never matches the baseline.

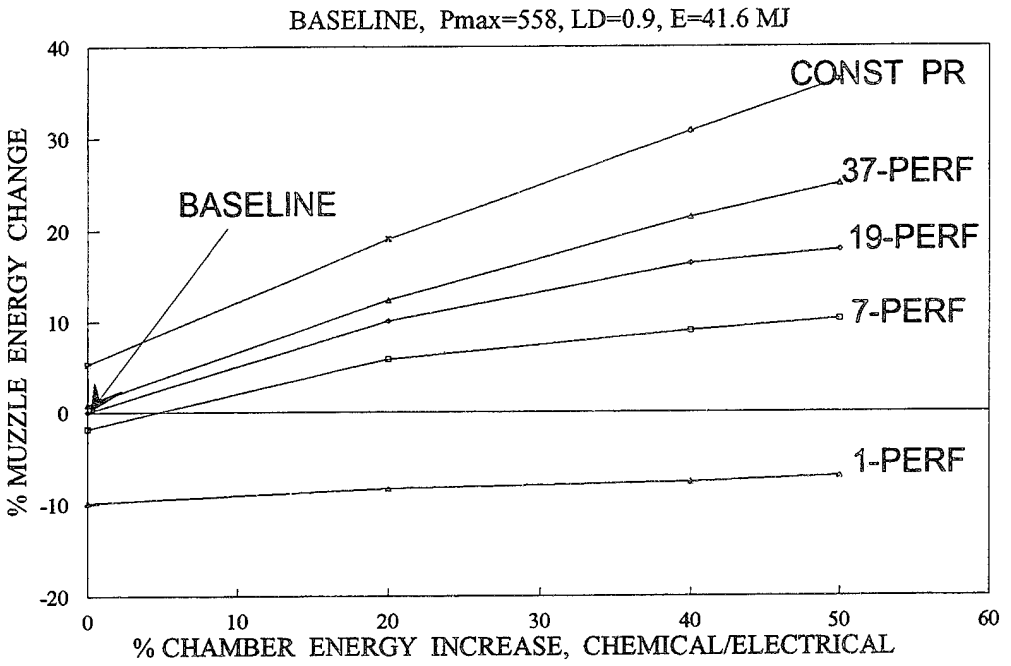

Figure 7. Potential performance change with chemical/electrical energy increase.

Table 3. Propellant Mass Fraction (Z) Burned at Muzzle Exit for Chamber Energy Increase

Energy Increase (%)	37 perf (Z)	19 perf (Z)	7 perf (Z)	1 perf (Z)
0	1.00	1.00	1.00	1.00
20	1.00	1.00	0.99	0.88
40	1.00	1.00	0.97	0.78
50	1.00	0.99	0.94	0.73

There is an improvement in the percent muzzle energy increase over the loading density data in Figure 2 because only the temperature T is increased with an increase in chemical/electrical energy. But with the increase in loading density, the free volume V is decreased *and* the mass, m, is increased which results in a greater reduction requirement in surface area (equations 1–3). Table 4 shows the propellant web (thickness of propellant between perforations, Figure 1) required for the data shown in Figures 2 and 7.

As was discussed earlier, as the web is increased, the overall grain size increases, which results in a decrease in surface-to-volume ratio. Hence, for a given mass of propellant, the *total* propellant surface area will decrease as the web is increased. Thus, as either the LD or propellant energy is increased, the web must also be increased, leading to a decrease in total propellant surface area and a resultant lowering of gun efficiency. Figure 8 illustrates the data from Table 4 columns 3 and 8, the web change as a function of percent increase of LD, and energy for a 19-perf grain geometry.

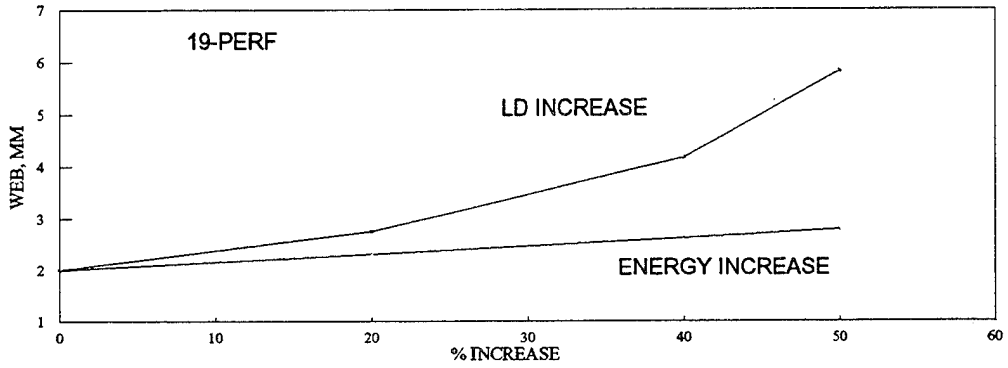

Figure 8. Web change for 19-perf geometry.

Table 4. Propellant Web Requirements for Increased LD and Propellant Energy

LD Increase (%)	Web				Energy Increase (%)	Web			
	37-perf (mm)	19-perf (mm)	7-perf (mm)	1-perf (mm)		37-perf (mm)	19-perf (mm)	7-perf (mm)	1-perf (mm)
0	1.90	2.01	2.02	2.80	0	1.90	2.01	2.02	2.80
20	2.47	2.76	2.92	4.44	20	2.15	2.31	2.37	3.39
40	3.35	4.18	4.71	7.93	40	2.40	2.62	2.73	4.03
50	4.20	5.83	6.90	12.3	50	2.52	2.79	2.90	4.36

It should be noted that the baseline reference point calculation uses a chemical energy of 41.6 MJ. Suppose that electrical energy in the form of a plasma were used exclusively to increase the muzzle energy. Examination of Figure 7 indicates that if a 23% increase in muzzle energy were desired, then a

50% increase in input energy would be required with a 37-perf grain configuration. A power supply in excess of 20 MJ would also be required, which would be too large for a mobile tank gun system. Thus, although increasing propellant energy by using electrical energy input would be beneficial, increasing the loading density must *also* be considered for energy enhancement to achieve increased performance. Additionally, as is shown in section 3.1, to achieve a significant performance increase from high loading densities, methods to operate at near ideal performance must be developed.

To summarize, at the present and in the foreseeable future, increases in chemical energy density or impetus will probably not exceed 10–20%. As seen in Figure 7, this would yield at best a 5–10% increase in muzzle energy.

4. REALIZING PERFORMANCE IMPROVEMENT FOR HIGH LOADING DENSITIES

The key to approaching the ideal (constant pressure) performance is to increase the energy generation rate after the maximum pressure is attained in the gun. From equations 1 and 2, this can be accomplished by increasing the surface area S, the temperature T (the propellant chemical energy density), or the burn rate r, *after* the maximum pressure has been reached. This problem has been addressed from the propellant surface area and propellant formulation (burn rate differentials) standpoint by Robbins and Worrell (1992). It is informative to find out what increase in burn rate is required to approach ideal performance for different grain geometries. The results of the calculations for pressure vs. time for the 7-perf propellant at +20% LD are shown as (1) in Figure 9. The percent muzzle energy changes relative to the baseline M829A1 charge are also shown. The burning rate coefficient, "b," in equation 3 was allowed to vary linearly from "b," at peak pressure (2.65 ms), up to "2b" at 4.45 ms. The burn rate coefficient then remained at "2b" until burnout. The effect of the change in burn rate on the pressure time history is shown as (2) in Figure 9. All propellant was consumed prior to the projectile exiting the tube. The muzzle energy increase has substantially improved and is approaching the ideal constant pressure value (+12.4%) for this LD.

When similar calculations were carried out for the 1-perf granulation propellant, a coefficient of "3b" was required to improve the performance. The surface area for the 1-perf propellant does not increase with mass fraction burned as does the 7-perf geometry, requiring a much larger increase in burning rate to yield the needed gas generation rate. On the basis of Figure 2, it is expected that the increase in burn rate required for 19- and 37-perf propellants will be less than 2b.

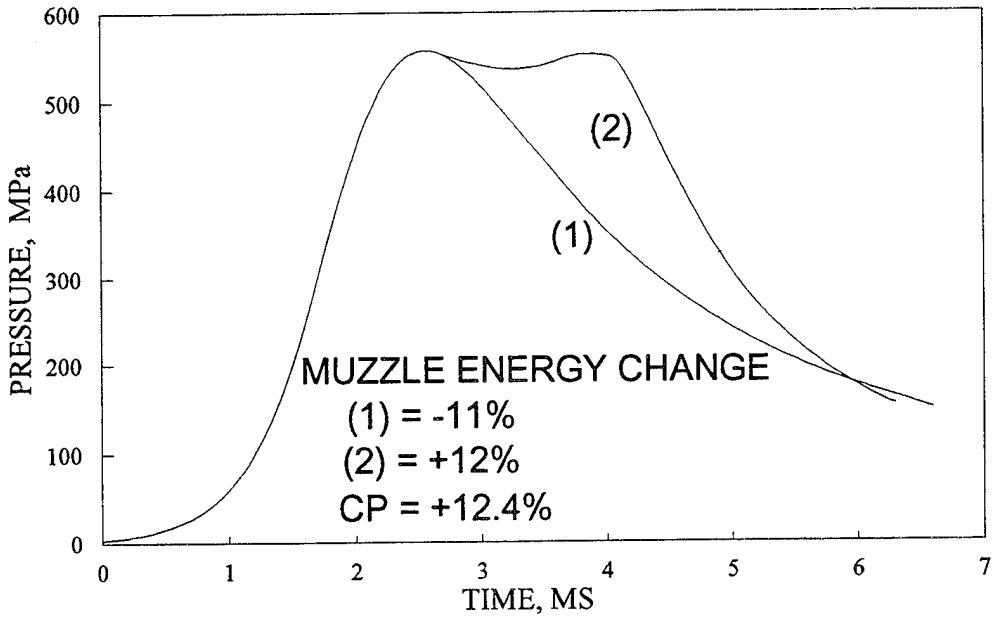

Figure 9. Effect of burn rate increase; 7-perf, LD = +20%.

The conclusion from this study is that performance improvement can be achieved by going to higher loading densities, but enhanced energy (mass) generation rates are required to realize that improvement (i.e., to operate near ideal pressure profiles). The next section describes how the ETC concept may be used to achieve this.

It should be noted that although this work focuses on an effort to use electrical energy to achieve the burn rate progressivity required to exploit high loading density charges, the burn augmentation has been addressed by Robbins and Worrell (1992) through a fast core concept wherein two layered propellants have the required burn rate differential. This problem has also been addressed through the use of deterrent layers on the outside of ball propellant (Gonzalez et al. 1989), which is used to inhibit the burn rate during the early stages of combustion. In this way, normalized rates of energy release as a function of weight fraction burned (progressivities) that are even in excess of that of the 37-perf propellant have been achieved (Gonzalez et al. 1989). Although problems have been encountered with this technique in reduced propellant energy, repeatability of ballistics, and propellant chemistry, further work in this area is being pursued with new propellant formulations (Olin Ordnance 1994).

5. ETC PROPULSION

The ETC propulsion concept is shown in the block diagram in Figure 10. Basically, in this example, a power supply is used to charge a capacitor-based energy storage device that also acts as a pulse-forming network (PFN). The network is used to generate a high-energy discharge in a plasma tube. The discharge of the plasma tube deposits the energy in the gun chamber. Over the last few years, a number of alternate designs have arisen, but the basic concept is to add electrical energy in the form of a plasma to the gun chamber in a preprogrammed manner. Various investigators have proposed different propellants in the form of liquids and slurries (Chiu and King 1993; Juhasz et al. 1993). The work discussed here concentrates on using the ETC concept with conventional solid propellants. The previous section demonstrates that to realize the performance improvement at high loading densities, the energy generation rate must be increased after maximum pressure. Can this be accomplished with electric energy by either directly adding energy after the maximum pressure or by altering the energy generation rate through an increase in the propellant burn rate after maximum pressure?

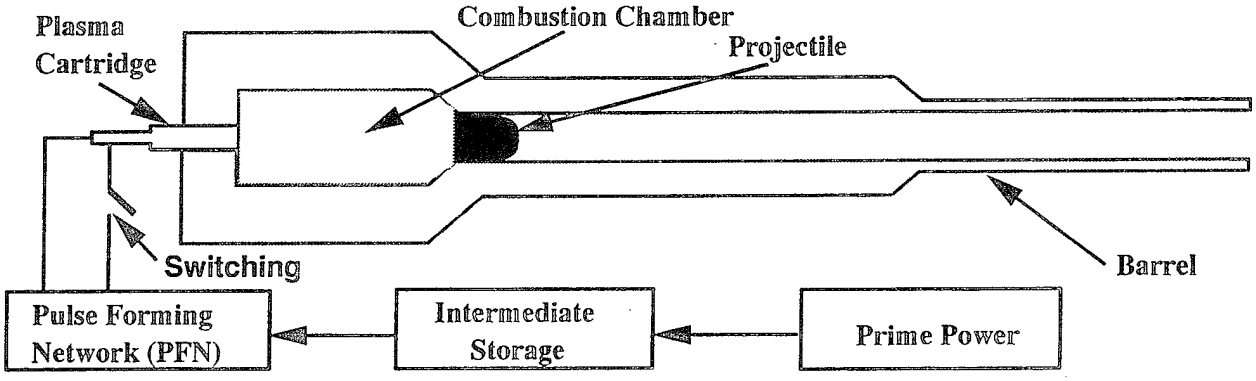

Figure 10. ETC gun concept.

5.1 Direct Addition of Electrical Energy. In Figure 2, one of the calculations carried out was for the 19-perf propellant geometry with a +20% increase in loading density. The pressure-time history for this calculation is plotted as curve (1) in Figure 11. The muzzle energy was 4% less than the baseline calculation. The constant pressure calculation for this loading density gave a muzzle energy increase of 16%.

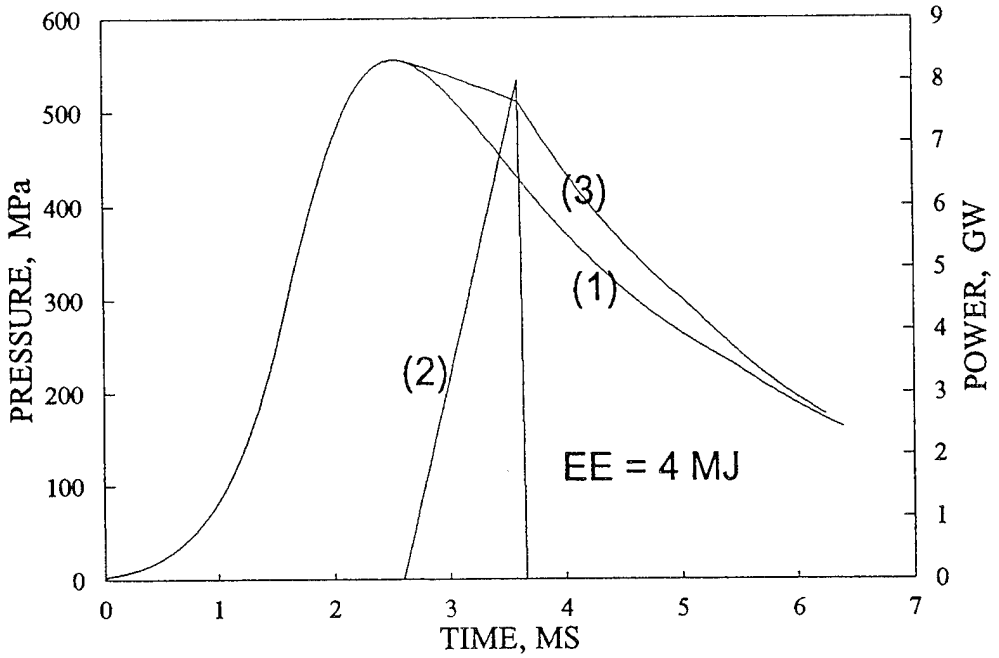

Figure 11. Effect of adding electrical energy on performance; (1) P-t for 19-perf, +20% LD, (2) electrical power (4 MJ), (3) P-t for 19-perf, +20% LD, +4 MJ electrical energy.

A calculation was now carried out in which electrical energy (4 MJ) was added after the maximum pressure. The linear power history is shown as (2) in Figure 11. The resultant pressure history is shown as (3). This calculation yielded a +7.6% increase over the baseline calculation. Compare this to the +16% for the CP calculation, *without* electrical energy (see Figure 2). These results are not necessarily optimum, but it is clear that post-maximum pressure addition of electrical energy shows improvement. Other calculations using an electrical pulse of 12 MJ and 12 GW yielded a muzzle energy increase of 18%, which, for current pulse power technology, would require power supply too large for vehicle integration.

5.2 Modification of Propellant Burn Rate With Electrical Energy. As discussed in section 4, a more efficient use of the propellant energy at the high loading densities can be achieved by increasing the burn rate after maximum pressure. It is known that propellant burn rate is affected by the initial ambient temperature of the propellant. Both theory (Glick 1967) and experiment (Juhasz, Doali, and Bowman 1981) have shown that the burn rate change with grain temperature is anywhere from 0.2 to 0.4 %/K for M30A1 propellant. In fact, Juhasz, Doali, and Bowman (1981) have indicated that the burning rate change may be substantially higher at pressures over 200 MPa and 373 K, although reliable data are not available.

Experience with gun firings has shown that JA2 propellant may have a temperature sensitivity double that of M30A1 propellant (i.e., up to 0.8 %/K) (Robbins 1994). These numbers indicate the type of burn rate change that can be expected with propellants burning at elevated initial temperatures. In the ETC gun concept, the electrical energy is converted into a plasma and enters, mixes, and envelops the propellant bed. The plasma temperature (>10,000 K) (Beyer and Bunte 1990) is much higher than JA2 propellant flame temperature of about 3,400 K, which is one of the highest flame temperatures of all common gun propellants. High-speed films (discussed later) have shown that the hot plasma envelops the propellant bed. What might be the bulk temperature rise of the propellant due to radiation absorption during the several-millisecond duration of the plasma pulse? As first suggested by Robbins (1994), could this temperature rise produce an increased burn rate that could be used to increase the gun efficiency?

Plasmas are optically dense media that behave nearly as a black-body radiator. The total radiation flux from a black body varies as T^4, and for a flame at temperatures of 3,000 K, it has a value of 450 W/cm^2. For the plasma at a temperature of 10,000 K, the flux is 56,600 W/cm^2. Figure 12 shows the well-known spectral energy distribution for black-body temperatures of 4,000, 6,000, and 10,000 K. Table 5 shows a quantitative breakdown of the energy flux over the infrared, visible, and ultraviolet (uv) spectral regions. Clearly for the plasma temperatures, the visible spectra (0.3–0.8 μm) are dominant. Most of the radiation energy occurs in this region, although there is also significant energy in the ultraviolet region. It is also obvious from Table 5 why plasma radiation (10,000 K) may be significantly more important in a ballistic event than radiation from JA2 propellant (~3,400 K) as the radiation is nearly two orders of magnitude larger.

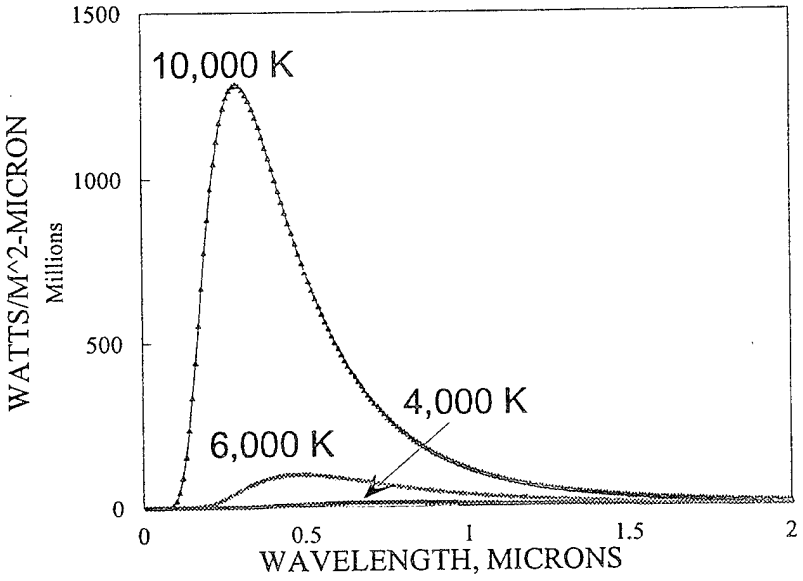

Figure 12. Black-body radiant flux distribution at 4,000, 6,000, and 10,000 K.

Table 5. Radiation Flux Spectral Distribution for Black Bodies at Various Temperatures for Infrared, Visible, and Ultraviolet Spectral Intervals

Temp. (K)	Total Flux (W/cm^2)	Infrared (near) Flux 0.8–2 μm (W/cm^2)	Visible Flux 0.3–0.8 μm (W/cm^2)	Ultraviolet Flux 0.0–0.3 μm (W/cm^2)
3,000	450	270	66	0.05
4,000	1,440	780	460	3.6
6,000	7,300	2,500	4,200	310
10,000	56,600	7,200	33,000	16,000
11,000	82,900	8,600	44,000	29,000
15,000	287,000	14,200	106,000	165,000

A radiation transport program (Cohen et al. 1993) was used to calculate the temperature profiles of a semi-infinite inert slab subjected to the radiation flux of a 10,000-K radiator such as a plasma, as a function of time and distance into the slab. To carry this out, the optical absorption properties of the propellant must be known. Cohen et al. (1993) have measured the extinction coefficient for JA2 at 1.06-μm wavelength. The values found varied from 4 to 21 cm^{-1}, mainly due to the uncertainty of scattering effects. Measurements were also made with an optical densitometer in the visible region and gave a value of 13 cm^{-1}. The results for the transport calculations are shown in Figure 13, with radiation flux from a plasma of 1-ms duration with an assumed temperature of 10,000 K. After a pulse of 1 ms, the temperature is calculated to increase by 175 K at a depth of 200 μm. The model assumes that the radiation is absorbed only in the solid slab. In the case of a burning propellant, it is possible that combustion products could absorb some of the radiation. Excluding particulate matter, most of the absorption from the gas-phase combustion products should occur in the infrared region. Approximately 13% of the radiation of a 10,000-K black body occurs between wavelengths of 0.8 and 2 μm (Table 5 and Figure 12). Absorption of this percentage of radiation by the gas products would not greatly affect the results. There is further evidence that absorption of visible radiation by combustion products is not significant. Burning propellants have been examined optically in numerous experiments, and the surface is clearly visible. Strong optical absorption would make this observation difficult.

The bulk temperature increase due to the plasma coupled with the burn rate temperature sensitivity range for JA2 (~0.3–0.8 %/K) would lead to burning rate increases of up to 50–140%. As was discussed

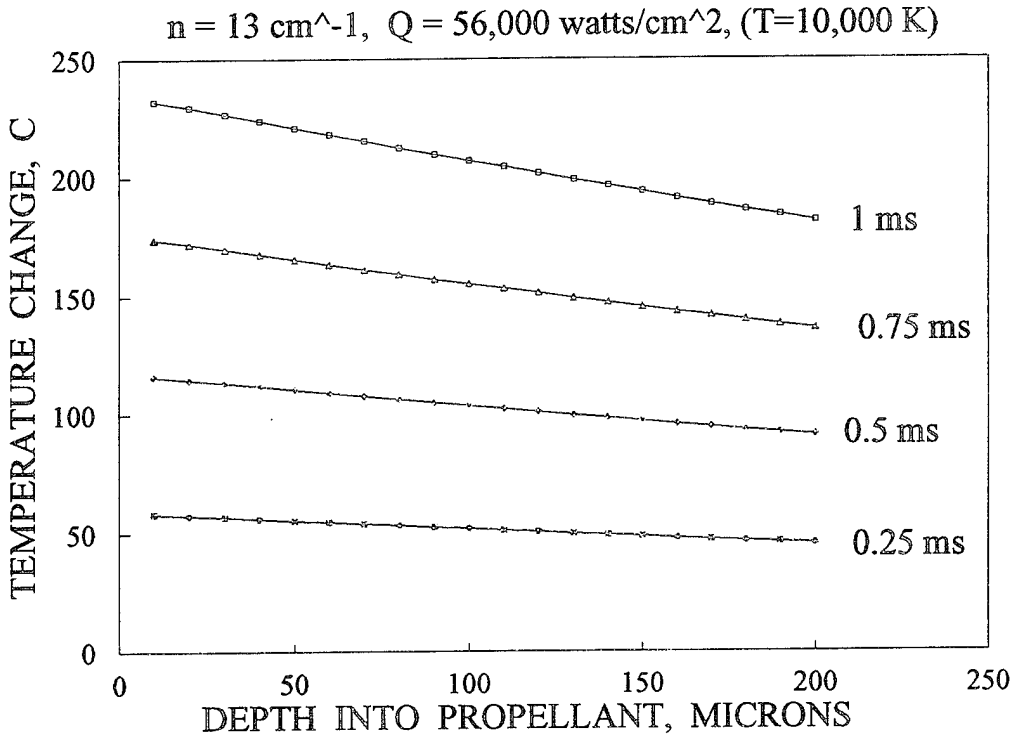

Figure 13. Temperature profiles of a propellant due to radiation flux.

earlier, a factor of 2 change in burn rate after the maximum pressure would significantly improve performance for a 7-perf grain geometry (Figure 9). In contrast to these calculations, Figure 14(a) shows the temperature rise of a slab due to radiation from a black body of 3,000 K, radiation that would be present from a propellant flame. The temperature rises are insignificant. Figure 14(b) illustrates the effect of the propellant absorption coefficient. Here the absorption coefficient has been raised by a factor of 10 to 100 cm^{-1} with a radiation temperature of 10,000 K. The temperature rises very rapidly but mainly at the surface and not very deeply in the interior of the propellant. Since the objective is to have the temperature rise *after* the maximum pressure, it is important that the *interior* of the grain rise in temperature since this is the region of the grain that will burn after the maximum pressure. In a practical case, the grain remains "hot" after the maximum pressure. Calculations also show that if the absorption coefficient is significantly less that 10 cm^{-1} there will be only a small and insignificant temperature rise. We have seen from Figure 13 that, for a propellant with the appropriate absorption properties, it is possible to achieve a significant temperature rise within the body of the propellant. This temperature rise coupled with the propellant combustion rate temperature sensitivity could cause significant changes in burn rate during the ballistic cycle.

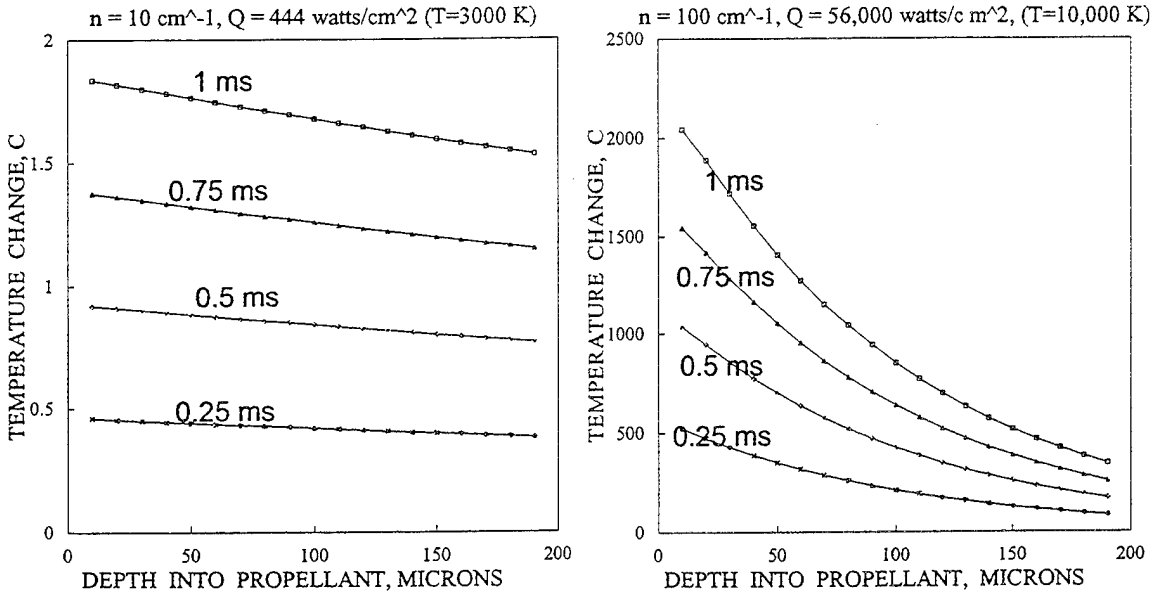

Figure 14. Temperature profiles: (a) effect of 3,000-K black-body temperature; (b) effect of propellant optical absorption coefficient × 10.

However, there are many practical problems in implementing this idea (e.g., introducing the plasma energy at the correct time in the ballistic cycle and ensuring that the temperature rise penetrates deeply enough into large grain propellants). Additionally, the temperature rise will be limited by the fact that the propellant surface is regressing while the heating is taking place and will move into the radiativelypreheated region of the unreacted propellant. This will depend on the grain geometry and operating pressure. Thus, although the calculations with this mechanism show the correct order of magnitude to achieve the necessary burn rate changes, experiments will be required to demonstrate the practical realization of the phenomenon.

The total electrical energy required to heat up the entire propellant bed should be considered. The M829A1 charge contains 7.9 kg of propellant. It would require approximately 1 MJ of electrical energy to raise the temperature of this amount of propellant 100 K. Although all of the parameters of the problem are of the right order of magnitude, experiments must be carried out to demonstrate the mechanism's impact on the burning rate and ballistic performance.

A further application of propellant heating should be mentioned. Because of the burn rate temperature sensitivity, cartridges are designed to operate under the maximum pressure at the highest operating temperatures, +50° C. Consequently, when the gun is fired at lower ambient temperatures, the performance will be reduced. Concepts are being considered for preheating charges in order to recover

this performance. The heating by the plasma during the ignition phase has shown to beneficially influence the ballistic temperature coefficient (U.S. Army Space and Strategic Defense Command 1992).

The analysis previously described is based on the assumption that the plasma temperature is approximately 10,000 K. Table 5 indicates that both the total radiation and the spectra distribution have a strong dependence on the temperature. At 10,000 K there is twice as much energy in the visible as in the uv region. However, if the temperature were 15,000 K, there would be significantly more uv radiation energy than in the visible. Other mechanisms may come into play since uv is known to be absorbed by combustion products. It is possible that burn rates could be influenced by this interaction. This is not a subject for study for this present work, but should be examined in future research on the interaction of the plasma with the propellant.

6. EXPERIMENTAL EVIDENCE OF PLASMA MODIFICATION OF BURN RATE

6.1 Direct Interaction of Plasma With a Propellant. Experiments were conducted at North Carolina State University (Edwards, Bourham, and Gilligan 1995) to study the interaction of plasma with propellants. Their plasma source is powered by a 17-kJ PFN. It was shown that plasma ignition of JA2 propellant with a 400-μs pulse increased burn rates by a factor of 5 when compared with conventional ignition and burning. Results of these experiments are shown in Figure 15. The geometry of the experiment was such that there was a strong flow of the plasma perpendicular to the surface of the propellant. Although the plasma flow was normal to the burning surface, it is not clear if any erosive effects were introduced by the plasma flow.

6.2 60-mm ETC Gun Firings. Based on anomalies in attempting to match experimental solid propellant ETC 60-mm gun firings results with interior ballistic simulations, there is some evidence that a plasma may affect propellant burn rates. Table 6 gives the gun firing results along with the interior ballistic calculations. It is seen that the burn rate coefficient (column 2) had to be increased by over 20% to approximately match the experimental pressure and velocity (Oberle et al. 1993; Robbins and Rosenberger 1993).

6.3 30-mm, Disk-Propellant, ETC Gun Firings. Test firings were performed at the U.S. Army Research Laboratory (ARL) in a 30-mm gun fixture and a 30-mm simulator with chamber volume (Katulka et al. 1993; Stobie et al. 1993), projectile mass and travel scaled to the 120-mm M256 cannon

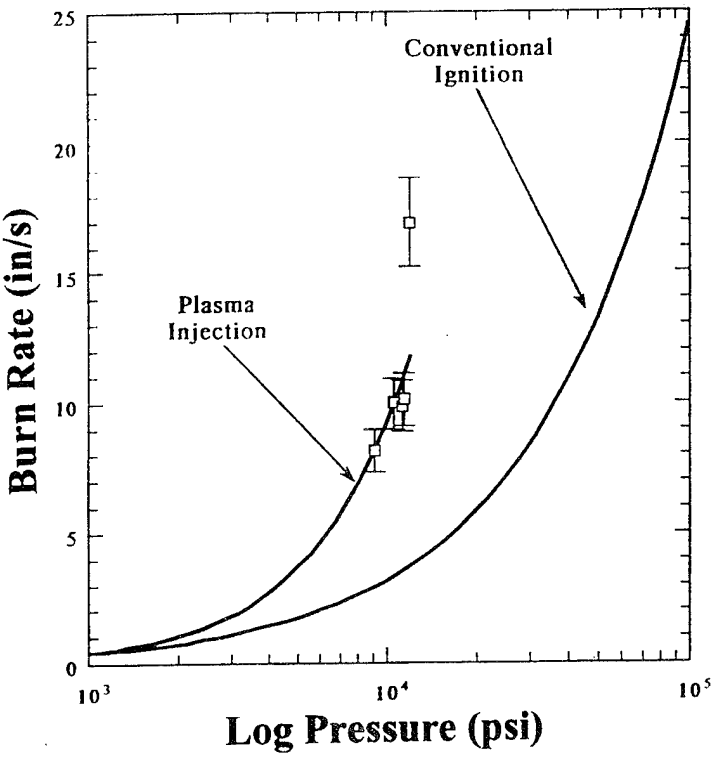

Figure 15. Effect of plasma on JA2 burn rate.

Table 6. Increasing Burn Rate to Effect a Ballistic Match for 60-mm ETC Gun

	Burn Rate Coefficient (m/s)	Exponent	Change (%)	Velocity (m/s)	Pressure (MPa)
Experiment 60-mm	—	—	—	1,040	400
Calculation	0.03612	1.075	0	876	294
	0.04153	1.075	15	1,002	348
	0.04587	1.075	27	1,124	403
	0.04696	1.075	30	1,154	420

using plasma augmentation of a JA2 charge of disk propellant (Robbins and Worrel 1992). The propellant is in the form of disks with axial holes similar to "washers." These are stacked together to form a very high loading density charge. A photograph of the windowed 30-mm gun simulator with the propelling charge is shown as (a) in Figure 16. Tests were carried out in this simulator with this charge

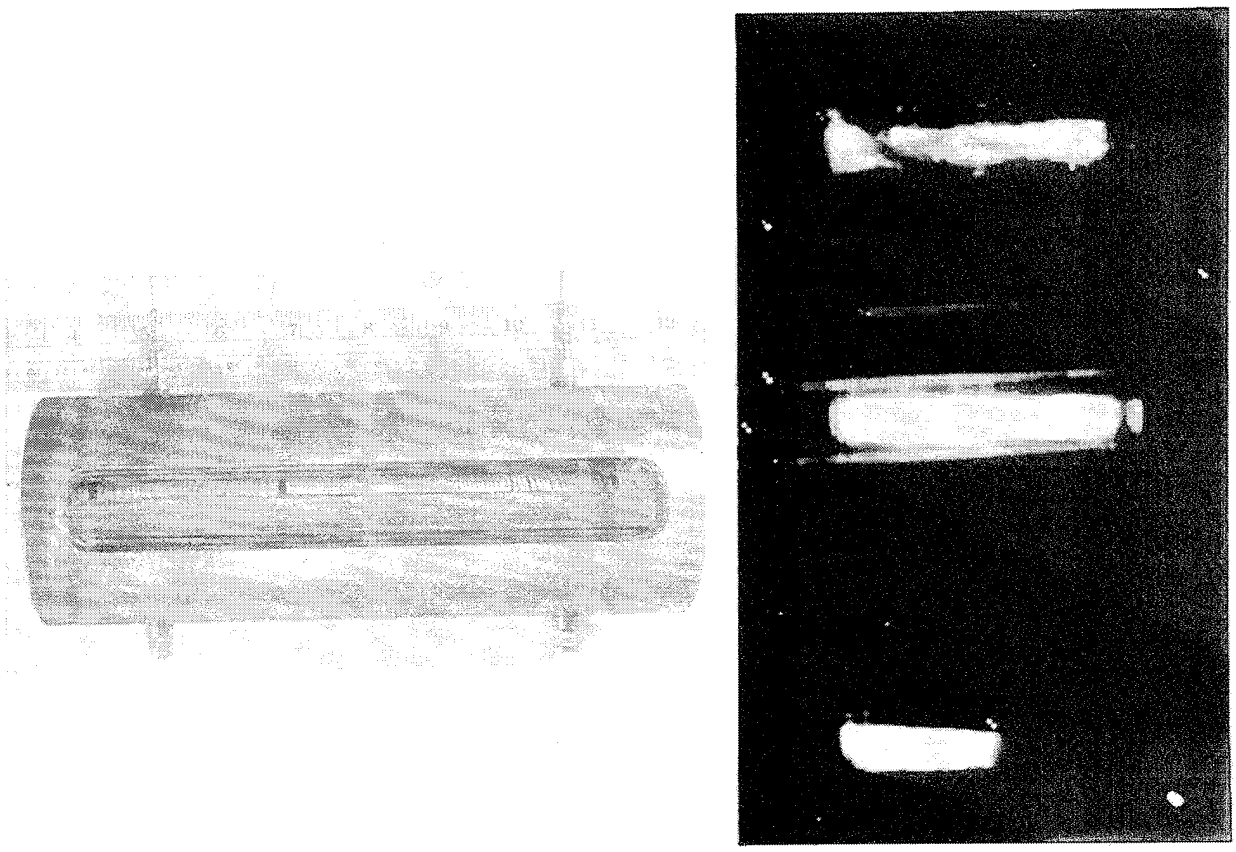

(a) (b)

Figure 16. (a) 30-mm simulator; (b) plasma-propellant interaction at 201, 160, and 92 μs (top to bottom).

configuration to study the interaction of the plasma with the propellant. The plasma was injected axially into the end of the chamber.

A slotted polyethylene centercore tube, coaxial with the chamber, was used to guide the plasma down the axis of the charge and, subsequently, radially into the propellant bed. A high-speed electronic camera was used to record the interaction of the plasma with the propellant bed. The results at three different times are shown as (b) in Figure 16; clearly the plasma envelops the entire propellant bed. Plasma can be seen entering between the propellant disks, a requirement discussed in section 5.2. Having established that a substantial portion of the propellant bed has been exposed to the plasma radiation, a similar charge

configuration was set up in a 30-mm gun fixture. The gun chamber and tube pressures were recorded along with muzzle velocities. The charge configuration was the same as that shown as (a) in Figure 16. For some tests, a chemical centercore igniter was used in place of the plasma centercore tube. The purpose of these tests was to have a direct comparison of a chemically- and ETC-ignited charge of the same configuration and composition. The experimental results were compared with interior ballistic calculations. The chemical igniter tests were used to establish baseline conditions for the calculations such as propellant burn rates, projectile shot start, and resistance profiles and heat losses. The ETC firings used the same parameters with the addition of electrical energy. If the calculations did not agree with the experiments, a parametric variation of ballistic conditions was carried out to fit the data. For the ETC tests, the configuration shown as (a) in Figure 16 was used. The results of the test firing and the interior ballistic calculations carried out to simulate the tests are shown in Table 7 and Figure 17.

Table 7. 30-mm ETC and Conventional Gun Firings and IB Calculations

Test, ID	Electrical Energy (kJ)	Pressure (MPa)	Velocity (m/s)
Conventional Ignition 30-mm Firings			
Experiment, 0330941	—	84	677
Experiment, 0330942	—	86	682
Calculation, 03309410	—	87	667
ETC 30-mm Firings			
Experiment, 032594	41	117	741
Experiment, 032894	40	119	751
Calculation, 03259410	36.8	147	797
Calculation, 03259413	18.4	117	736
Calculation, 03259419	36.8	120	743

For the conventional igniter tests, the calculations used burn rates for JA2 with the exception that the low pressure (<70 MPa) burn rate coefficient (Calculation 03309410) had to be lowered from 3.589 to 3.30 mm/s to match the experimental results. This is not unreasonable as the burn rate derived from closed chamber results is not very well determined at pressures below 100 MPa. This burn rate and all

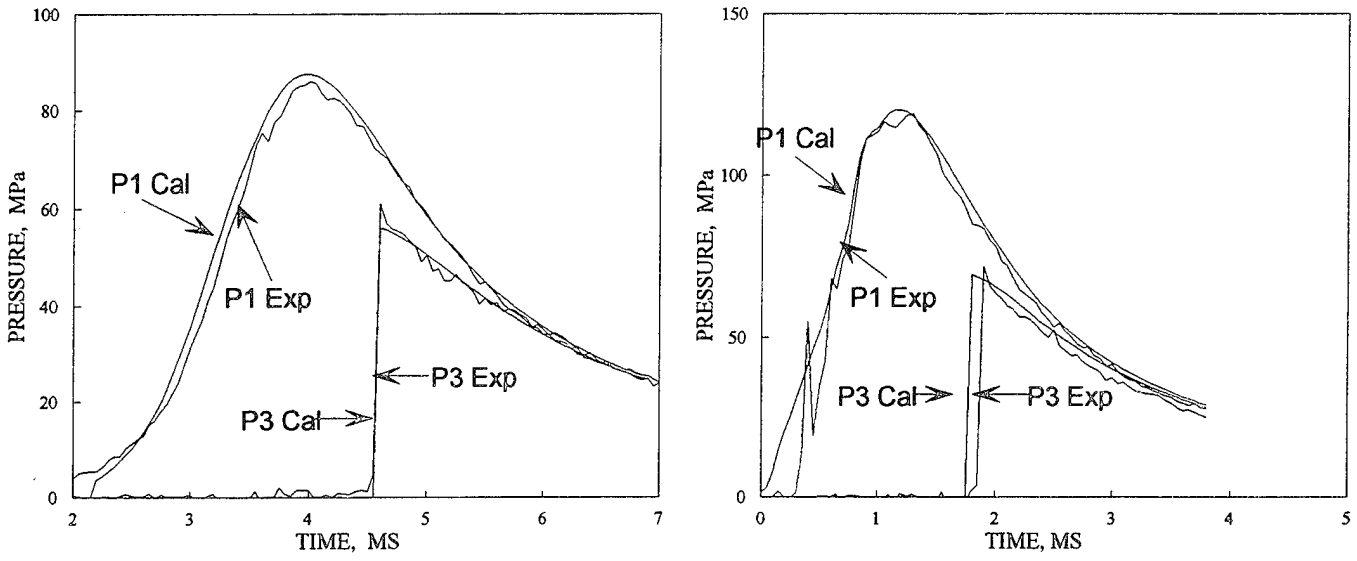

Figure 17. Comparison of experimental and calculated P-t histories for (a) conventional ignition (exp., 0330941; cal., 03309410) and (b) ETC ignition (exp., 032594; cal., 03259419): P1, chamber gauge, P3 tube gauge.

other parameters were then held fixed for the ETC calculations shown in Table 7 (Calculation 03259410) which, of course, included the electrical energy input. The calculated pressure and velocity were too high compared with the experiment. Many calculations were carried out in an effort to match the data. Calculation 03259413, shown in Table 7, used 1/2 the measured input power. The agreement with the experiment was good. The assumption made in ETC firings is that all the measured electrical energy goes into the propellant product working fluid. This calculation may be indicating that this is not the case and that there are losses (higher than normal convective or radiative) not considered. For the final calculation (03259419, Figure 17[b]), 30% of the propellant was delayed in ignition until after Pmax. The calculated results are in reasonable agreement with experiment. This computation suggests some kind of delayed ignition of the propellant due to a nonuniform plasma distribution within the propellant bed.

Summarizing, the results for this plasma/disk propellant gun firings are too ambiguous to determine the effect of the plasma on burning of the propellant. It may be that the disk propellant configuration is exhibiting some unusual flow or combustion effect. Anomalous behavior of the disk propellant has been observed in 120-mm gun firings carried out by Robbins (1994). More tests will be required at higher energy and longer plasma pulses to test the concept. Meanwhile, current efforts will be concentrated in further closed chamber tests to be discussed in section 6.5.

6.4 30-mm, Monolithic-Grain, ETC Gun Firings. Very high loading densities can be achieved by using monolithic propellant grains. Some tests were carried out (Harris et al. 1993) using a monolithic grain configuration in a 30-mm gun test fixture. The grain was in the form of a right circular cylinder with an outside diameter of 28 mm and an inside diameter of 6.1 mm. It was mounted in the chamber, and the plasma energy was introduced axially down the 6.1-mm hole that ran the length of the propellant cylinder. With this configuration, the entire inner surface of the grain was subjected to the high velocity flow and radiation from the plasma. Chamber pressures, projectile muzzle velocities, and electrical power input were recorded. Interior ballistic calculations were carried out using the IBHVG-ETC code in an effort to simulate the ballistic results.

Selected experimental data and calculations are given in Table 8. It is seen that the calculations underpredict the muzzle velocity measured experimentally. This is very evident for Test 22. Lieb and Gillich (1994) have conducted a post-mortem analysis on propellant grain fragments recovered from the 30-mm gun firings. The scanning electron microscopy technique was applied to various surfaces of the fragments, and the resulting micrographs provided considerable insight into the possible combustion mechanisms. Analysis of the photographs indicated the presence of erosive burning, microdeconsolidation, and in-depth combustion, each of which could augment propellant mass generation rate. Although other interpretations are possible (Leib and Gillich 1994), the in-depth combustion can be interpreted as coming from in-depth radiation absorption that raised the temperature at which chemical reactions occurred and caused an increase in burn rate.

These interpretations lend some support to the radiation heating model proposed in section 5.2. It should also be mentioned that propellant discs recovered from the 30-mm gun firings described in section 6.3 also showed similar effects as those described previously.

6.5 Closed Chamber Tests. Closed chamber tests were carried out (Oberle and DelGuercio 1994) on the JA2 disk propellant, with the plasma injection and propellant configuration similar to that described in section 6.3. The important difference between the closed chamber and the gun tests is that in the closed chamber, there is no down-bore motion; hence the propellant will not move out of the plasma plume. This propellant movement could possibly happen in the gun configuration, reducing the effectiveness of the plasma interacting with the entire propellant bed during the duration of the pulse. The closed chamber pressure time-data along with the electrical power input have been reduced to the characteristic log of burn rate vs. log of pressure data shown in Figure 18. The solid straight line is a representation of the

Table 8. Monolithic Grain ETC Results, Experiment and Calculation

1/2-length charge, 90 g			Experiment		Calculations	
Test No.	EE (kJ)	EE Den (kJ/g)	Pmax (MPa)	v (m/s)	Pmax (MPa)	v (m/s)
21	30	0.36	34	245	40	178
22	57	0.69	110	617	58	249
23	45	0.53	110	596	—	—
24	18	0.21	27	173	—	—
25	30	0.36	34	240	—	—
26	15	0.18	40	310	—	—
27	27	0.32	120	520	—	—

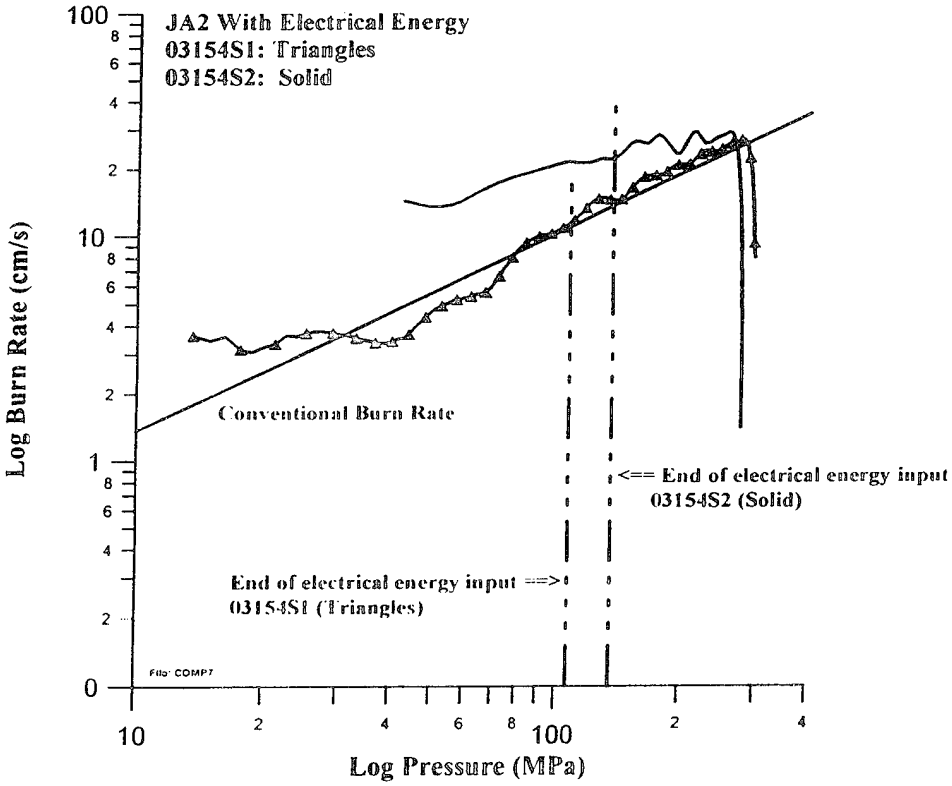

Figure 18. Burn rate of JA2 with plasma interaction.

conventional JA2 burn rate. Two ETC tests are illustrated, 03154S1 (triangles) and 03154S2 (solid). The pressure at which the electrical pulse was terminated is also shown. The results are ambiguous; S2 indicates a 30% increase in burn rate, but S1 does not show a significant difference. Closed chamber tests are continuing using a variety of electrical pulses designed to resolve this ambiguity.

7. SUMMARY AND CONCLUSIONS

The analysis presented here indicates that two factors are necessary to increase performance within a given gun envelope—increased propellant energy and operating at or near the ideal constant pressure gun conditions. Increased energy can be attained using increased loading density, new, higher energy propellant formulations, or additional electric energy, in the form of a plasma, during the interior ballistic cycle. For the near term, using solid propellants, the last two of these methods *by themselves* are impractical, either because developing new, significantly more energetic solid propellants is a difficult task or because electric power supply sizing issues are expected to remain with us for some time to come.

What remains, therefore, is to increase the energy in the chamber using high loading density charges of well-characterized, solid propellants. To make practical use of these, however, requires a high degree of burning progressivity to make use of the extra energy and to approach the ideal gun performance. While progressive grain design (19- or 37-perf grains) will permit the use of higher propellant loading densities, additional burning rate enhancement after maximum pressure is necessary to realize the near ideal performance. This could be attained by using chemical formulation methods such as deterrents or other layered propellant formulation techniques. It could also be accomplished by direct influence of plasma heating on the burning characteristics of the propellant.

The experimental demonstration of the effect of electrical energy on combustion is somewhat ambiguous at this time. If, however, further tests confirm the effect of plasma enhancement of burn rate then it may be possible to couple this effect to high grain progressivity and with the use of deterrents. This should permit effective use of high-density solid propellant charges in ETC propulsion concepts.

Finally, though only briefly discussed in this report, recent results obtained under an U.S. Army Space and Strategic Defense Command contract (Propulsion Physics Laboratory, Soreq Nuclear Research Center, Yavne, Israel) (U.S. Army Space and Strategic Defense Command 1992) indicate that plasma-augmented ballistics appear to be an effective way of reducing the ballistic temperature coefficient and possibly

operating the gun at its highest operating pressure at all temperatures. (At these higher pressures, it should be possible to take further advantage of progressivity increases in high-density charges.)

In summary, a combination of *all* the approaches discussed in this report will be required to give significant increases in performance (i.e., increases in loading density, propellant energy density, and electric energy input for energy augmentation; propellant burn rate control either chemically or through plasma effects; and elimination of temperature sensitivity). Assuming a loading density of 1.25 g/cm^3 (Koszoru 1994), specific energy of 1,380 J/g (20% increase for JA2), 4 MJ of electrical energy, and an operating pressure of 700 MPa under all ambient conditions—reasonable expectations for future values—a muzzle energy of 17.2 MJ, 56% above the baseline, could be expected if operation at near ideal (constant pressure) gun operation could be obtained. This will require not only innovative use of the electrical plasma but also substantial gains in propellant chemistry to aid in the necessary tailoring of propellant burn rates.

8. REFERENCES

Anderson, R. D., and K. D. Fickie. "IBHVG2-A User's Guide." BRL-TR-2829, U.S. Army Ballistic Research Laboratory, Aberdeen Proving Ground, MD, July 1987.

Beyer, R. A., and S. W. Bunte. "Spatial and Temporal Temperature Studies of ETC Plasmas." 27th JANNAF Combustion Subcommittee Meeting, vol. 1, CPIA Pub. 557, pp. 359–363, November 1990.

Chiu, D., and R. King. "Parametric Studies of Electrothermal Chemical (ETC) Candidate Propellants Using ARDEC 10-mm ETC Test Fixture." 30th JANNAF Combustion Subcommittee Meeting, vol. 4, CPIA Pub. 606, pp. 65–75, November 1993.

Cohen, A., K. McNesby, S. Bilyk, and A. Kotlar. "Optical Properties of Solid Propellants." 30th JANNAF Combustion Subcommittee Meeting, vol. 1, CPIA Pub. 606, pp. 295–304, November 1993.

Edwards, C. M., M. A. Bourham, and J. G. Gilligan. "Experimental Studies of the Plasma-Propellant Interface for Electrothermal-Chemical Launchers." 7th Electromagnetic Launch Symposium, to be published IEEE Transactions on Magnetics, January 1995.

Glick, R. L. "Temperature Sensitivity of Solid Propellant Burning Rate." AIAA Journal, vol. 5, pp. 586–587, 1967.

Gonzalez, A., D. Worthington, W. Aungst, and J. Newberry. "Ball Powder Propellants and Temperature Sensitivity." 26th JANNAF Combustion Subcommittee Meeting, vol. 1, CPIA Pub. 529, pp. 317–324, October 1989.

Harris, L. E., D. Chiu, J. Prezelski, P. O'Reilly, R. Marchak, D. S. Downs, W. F. Oberle, J. R. Greig, H. A. McElroy, and J. G. Buzzett. "Enhanced Propellant Burn Rate Through Plasma Erosion." 30th JANNAF Combustion Subcommittee Meeting, vol. 4, CPIA Pub. 606, pp. 121–135, November 1993.

Juhasz, A. A., H. A. McElroy, E. W. Schmidt, E. F. Rothgery, J. R. Greig. "The Search for Alternate ETC Propellants." 30th JANNAF Combustion Subcommittee Meeting, vol. 4, CPIA Pub. 606, pp. 77–107, November 1993.

Juhasz, A. A., J. O. Doali, and R. E. Bowman. "Wide Temperature Range Burning Rate Studies of M30A1 Propellant." 18th JANNAF Combustion Subcommittee Meeting, vol. 2, CPIA Pub 347, pp. 13–23, October 1981.

Katulka, G. L., T. Khong, K. Nekula, and K. White. "Plasma Characterization for Electro-Thermal Chemical Gun Applications." 30th JANNAF Combustion Subcommittee Meeting, vol. 4, CPIA Pub. 606, pp. 147–162, November 1993.

Koszoru, A. A. "Maximum Loading Density Study for 120-mm Charges Using Solid Cord, Scroll, and Slab JA2 Propellants." ARL-MR-129, U.S. Army Research Laboratory, Aberdeen Proving Ground, MD, March 1994.

Lieb, R. J., and C. J. Gillich. "Morphology of Extinguished Monolithic Grains Fired in a 30-mm SPETC Gun." 1994 JANNAF Propellant Development and Characterization Subcommittee Meeting, 13–15 April 1994, NASA Kennedy Space Flight Center, FL.

Oberle, W., and M. DelGuercio. Private Communication. U.S. Army Research Laboratory, Aberdeen Proving Ground, MD, 1994.

Oberle, W., A. Juhasz, D. Downs, T. Doran, J. Copley, and LTC S. Kee. "An Overview and Analysis of U.S. Efforts in Electrothermal-Chemical (ETC) Gun Technology." Proceedings of the 14th International Symposium on Ballistics, vol. 1, pp. 163–172, September 1993.

Olin Ordnance. "Electrothermal-Chemical (ET-C) Gun Alternate Working Fluid (Propellant) Systems Investigation and Study Effort." Semiannual Progress Report, Data Item A002, Contract DAAA15-90-C-1061, U.S. Army Ballistic Research Laboratory, Aberdeen Proving Ground, MD, 1994.

Robbins, F. W. Private Communication. U.S. Army Research Laboratory, Aberdeen Proving Ground, MD, 1994.

Robbins, F., and T. Rosenberger. Private Communication. U.S. Army Research Laboratory, Aberdeen Proving Ground, MD, 1993.

Robbins, F. W., and D. A. Worrell. "Fast Core Layered Propellant Study." 29th JANNAF Combustion Subcommittee Meeting, vol. 1, CPIA Pub. 593, pp. 91–98, October 1992.

Stobie, I., K. Nekula, K. White, G. L. Katulka, T. Khong, and W. Oberle. "Solid Propellant Electrothermal-Chemical Ballistic Studies in a 30-mm Fixture." 30th JANNAF Combustion Subcommittee Meeting, vol. 4, CPIA Pub. 606, pp. 109–120, November 1993.

U.S. Army Space and Strategic Defense Command. "Development of Electrothermal Launcher Technology for a Ballistic Missile Terminal Defense System." DASG60-92-C-0198, Huntsville, AL, 1992.

NO. OF COPIES	ORGANIZATION
2	ADMINISTRATOR ATTN DTIC DDA DEFENSE TECHNICAL INFO CTR CAMERON STATION ALEXANDRIA VA 22304-6145
1	DIRECTOR ATTN AMSRL OP SD TA US ARMY RESEARCH LAB 2800 POWDER MILL RD ADELPHI MD 20783-1145
3	DIRECTOR ATTN AMSRL OP SD TL US ARMY RESEARCH LAB 2800 POWDER MILL RD ADELPHI MD 20783-1145
1	DIRECTOR ATTN AMSRL OP SD TP US ARMY RESEARCH LAB 2800 POWDER MILL RD ADELPHI MD 20783-1145
	ABERDEEN PROVING GROUND
5	DIR USARL ATTN AMSRL OP AP L (305)

NO. OF COPIES	ORGANIZATION
1	COMMANDER ATTN SMCAR WAH T MR J DOMEN USAARDEC BLDG 62 NORTH PCTNY ARSNL NJ 07806-5000
1	COMMANDER ATTN SMCAR AEE BR MR K KLINGMAN USAARDEC BLDG 1501 PCTNY ARSN NJ 07806-5000
1	DIRECTOR ADV TECH CTR USA BMD PO BOX 1500 HUNTSVILLE AL 35807
1	CHAIRMAN DOD EXP SAFETY BD RM 856C HOFFMAN BLDG 1 2461 EISENHOWER AVE ALEXANDRIA VA 22331-0600
1	PM-PALADIN ATTN SFAE AR HIP IP R DE KLEINE PCTNY ARSNL NJ 07806-5000
1	COMMANDER ATTN AMSMC PBM E L LAIBSON USAARDEC PROD BASE MOD AGNCY PCTNY ARSNL NJ 07806-5000
3	PEO ARMAMENTS PM TMAS ATTN AMCPM TMA K RUSSELL AMCPM TMA 105 AMCPM TMA 120 PCTNY ARSNL NJ O7805-5000
2	DIRECTOR ATTN SARWV RD G CARAFANO R HASOENBEIN USA WATERVLIET ARSNL BENET LAB WATERVLIET NY 12189
1	DIRECTOR ATTN SARWV RD P VOTIS USA WATERVLIET ARSNL BENET LAB WATERVLIET NY 12189

NO. OF COPIES	ORGANIZATION
1	DIRECTOR ATTN SMCAR CCB R DR S SPOCK USA BENET LAB WATERVLIET NY 12189
3	COMMANDER ATTN AMSMC IRC G COWAN R ZASTROW SMCAR ESM R W FORTUNE USAAMCCOM ROCK ISLAND IL 61299-7300
1	COMMANDER ATTN ASQNC ELC ISL R R&D TECH LIB MYER CTR USACECOM FT MONMOUTH NJ 07703-5301
1	COMMANDANT ATTN AVIATION AGNCY USAAS FT RUCKER AL 36360
1	DIRECTOR ATTN ATCD MA MAJ WILLIAMS HQ TRAC RPD FT MONROE VA 23651-5143
1	HEADQUARTERS ATTN AMCICP AD M F FISETTE 5001 EISENHOWER AVE USAMC ALEXANDRIA VA 22333-0001
2	COMMANDER ATTN SMCAR CCD D SPRING SMCAR CCS USAARDEC PCTNY ARSNL NJ 07806-5000
2	COMMANDER ATTN SMCAR CCH T L ROSENDORG SMCAR CCH V E FENNELL USAARDEC PCTNY ARSNL NJ 07806-5000
2	COMMANDER ATTN SMCAR AEE B D DOWNS D CHIU USAARDEC PCTNY ARSNL NJ 07806-5000

NO. OF COPIES	ORGANIZATION
2	COMMANDER ATTN SMCAR AEE J LANNON SMCAR AED S KAPLOWITZ USAARDEC PCTNY ARSNL NJ 07806-5000
2	COMMANDER ATTN SMCAR FSA T M SALSBURY T GORA USAARDEC PCTNY ARSNL NJ 07806-5000
2	COMMANDER ATTN SMCAR B KNUTELSKY A GRAF K CHEUNG USAARDEC PCTNY ARSNL NJ 07806-5000
2	COMMANDER ATTN SMCAR EG G FERDINAND R ZIMANY USAARDEC PCTNY ARSNL NJ 07806-5000
2	COMMANDER ATTN TECH LIB D MANN USARO PO BOX 12211 RSCH TRI PK NC 27709-2211
1	COMMANDER ATTN STRBE WC TECH LIB VAULT USABRDC BLDG 315 FT BELVOIR VA 22060-5606
1	COMMANDER DEFENSE LOGISTICS STUDIES USA TRAC FT LEE FT LEE VA 23801-6140
1	PRESIDENT USA ARTILLERY BD FT SILL OK 73503
1	COMMANDANT USACGSC FT LVNWORTH KS 66027-5200

NO. OF COPIES	ORGANIZATION
1	COMMANDANT ATTN REV & TNG LIT DIV USASWS FT BRAGG NC 28307
1	COMMANDER ATTN SMCRA QA HI LIBRARY RADFORD ARMY AMMO PLANT RADFORD VA 24141
1	COMMANDANT ATTN STSF TSM CN USAFAS FT SILL OK 73505-5600
1	DEPUTY COMMANDER SDC ATTN SFAE SD HVL D LIANOS PO BOX 1500 HUNTSVILLE AL 35887-8801
3	COMMANDER ATN AMXST MC 3 S LEBEAU C BEITER 220 SEVENTH ST NE USAFSTC CHARLOTTESVILLE VA 22901
1	COMMANDANT ATTN ATSF CO MW B WILLIS USAFACS FT SILL OK 73503
1	OFFICE OF NAVAL RESEARCH ATTN CODE 473 R S MILLER 800 N QUINCY ST ARLINGTON VA 22217
2	COMMANDER ATN SEA 62R SEA 64 NSSC WASH DC 20362-5101
1	COMMANDER ATTN AIR 954 TECH LIB NSSC WASH DC 20360

NO. OF COPIES	ORGANIZATION
1	NAVAL RESEARCH LABORATORY TECH LIB WASH DC 20375
2	COMMANDER ATTN J P CONSAGA C GOTZMER NSWC SLVR SPRNG MD 20902-5000
2	COMMANDER ATTN CODE R13 K KIM CODE R13 R BERNECKER NSWC SLVR SPRNG MD 20902-5000
3	COMMANDER ATTN 6210 C SMITH 6210J K RICE 6210C S PETERS NSWC INDIAN HEAD DIV INDIAN HEAD MD 20640-5035
3	COMMANDER ATTN CODE G33 T DORAN J COPLEY CODE G30 G&M DIV NSWC DAHLGREN DIV DAHLGREN VA 22448-5000
3	COMMANDER ATTN CODE G301 D WILSON CODE G32 GUNS SYSTEM DIV CODE E23 TECH LIB NSWC DAHLGREN DIV DAHLGREN VA 22448-5000
1	COMMANDER ATTN CODE 4052 S BACKER BLDG 108 NSWC CRANE DIV CRANE IN 47522-5000
1	COMMANDER ATTN CODE 5B331 R S LAZAR TECH LIB NUSC ENG CONV DEPT NEWPORT RI O2840

NO. OF COPIES	ORGANIZATION
1	COMMANDER ATTN CODE 270P1 MR E CHAN 101 STRAUS AVE NSWC INDIAN HD DIV INDIAN HEAD MD 20640
1	COMMANDER ATTN CODE 3120 MR R RAST 101 STRAUS AVE NSWC INDIAN HD DIV INDIAN HEAD MD 20640
1	COMMANDER ATTN CODE 210P1 R SIMMONS 101 STRAUS AVE NSWC INDIAN HD DIV INDIAN HEAD MD 20640
2	COMMANDER ATTN CODE 6210 S BOYLES N ALMEYDA 101 STRAUS AVE NSWC INDIAN HD DIV INDIAN HEAD MD 20640
1	COMMANDER ATTN CODE 3891 A ATWOOD NAWC CHINA LAKE CA 93555
1	COMMANDER ATTN SMCAR CCH J HEDDERICH BLDG 1 USAARDEC PCTNY ARSNL NJ 07806-5000
1	OLAC PL TSTL ATTN D SHIPLETT EDWARDS AFB CA 93523-5000
10	DIRECTOR OFC OF CENT REF DISSEM BR CENTRAL INTELLIGENCE AGENCY RM GE47 HQS WASH DC 20502
1	DIRECTOR ATTN J E BACKOFEN CENTRAL INTELLIGENCE AGENCY HQ RM 5F22 WASH DC 20505

NO. OF COPIES	ORGANIZATION
2	DIRECTOR ATTN B KASHWHIA H DAVIS LANL LOS ALAMOS NM 87545
1	DIRECTOR ATTN MS L355 A BUCKINGHAM LLNL PO BOX 808 LIVERMORE CA 94550
1	DIRECTOR ATTN R ARMSTRONG DIV 8357 COMBUSTION RSCH FACILITY SANDIA NAT LAB LIVERMORE CA 94551-0469
1	DIRECTOR ATTN S VOSEN DIV 8357 COMBUSTION RSCH FACILITY SANDIA NAT LAB LIVERMORE CA 94551-0469
1	UNIV OF ILLINOIS ATTN PROF H KRIER 144 MEB DEPT OF MECH IND ENG 1206 N GREEN ST URBANA IL 61801
1	JHU CPIA ATTN T CHRISTIAN SUITE 202 10630 LTLE PATUXENT PKWY COLUMBIA MD 21044-3200
2	PENN STATE UNIV ATTN J BROWN DEPT OF MECHANICAL ENGR 312 MECHANICAL ENGR BLDG UNIVERSITY PARK PA 16802
1	NCSU ATTN J G GILLIGAN BOX 7909 1110 BURLINGTON ENGR LABS RALEIGH NC 27695-7909

NO. OF COPIES	ORGANIZATION
1	NSCU ATTN M BOURHAM PO BOX 7909 1110 BURLINGTON ENGR LABS RALEIGH NC 27965-7909
2	INSTITUTE FOR ADVANCED STUDIES ATTN DR H FAIR DR T KIEHNE 4030 2 W BAKER LANE AUSTIN TX 78759-5329
1	SRI INTERNATIONAL ATTN TECH LIB PROPULSION SCIENCES DIV 333 RAVENSWOOD AVE MENLO PARK CA 94025
1	SPARTA ATTN DR M HOLLAND 945 TOWNE CENTER DR SAN DIEGO CA 92121-1964
3	UNITED DEFENSE ATTN MR M SEALE DR A GIOVANETTI MR J DYVIK 4800 E RIVER RD MINNEAPOLIS MN 55421-1498
1	HERCULES INC RADFORD ARMY AMMO PLANT ATTN D A WORRELL PO BOX 1 RADFORD VA 24141
1	HERCULES INC ATTN E SANFORD RADFORD ARMY AMMO PLANT PO BOX 1 RADFORD VA 24141
2	GDLS ATTN MR F LUNSFORD DR M WEIDNER PO BOX 2074 WARREN MI 48090-2074

NO. OF COPIES	ORGANIZATION
3	OLIN ORDNANCE ATTN V MCDONALD LIBRARY H MCELROY D WORTHINGTON PO BOX 222 ST MARKS FL 32355
1	PAUL GOUGH ASSOC INC ATTN P S GOUGH 1048 SOUTH ST PORTSMOUTH NH 03801-5423
1	PHYSICS INTL LIBRARY ATTN H W WAMPLER PO BOX 5010 SAN LEANDRO CA 94566-05999
1	ROCKWELL INTL ATTN BA08 J E FLANAGAN ROCKETDYNE DIV 6633 CANOGA AVE CANOGA PARK CA 91304
1	ROCKWELL INTL ATTN BA08 J GRAY ROCKETDYNE DIV 6633 CANOGA AVE CANOGA PARK CA 91304
1	SCIENCE APPLICATIONS INC ATTN J BATTEH 1225 JOHNSON FERRY RD STE 100 MARIETTA GA 30068
1	SCIENCE APPLICATIONS INC ATTN L THORNHILL STE 100 1225 JOHNSON FERRY RD MARIETTA GA 30068
1	ELI FREEDMAN & ASSOC ATTN E FREEDMAN 2411 DIANA RD BALTIMORE MD 21209-1525
1	VERITAY TECH INC ATTN MR E FISHER 4845 MILLERSPORT HWY E AMHERST NY 14051-0305

NO. OF COPIES	ORGANIZATION
1	BATTELLE ATTN TACTEC LIB J N HUGGINS 505 KING AVE COLUMBUS OH 43201-2693
1	CA INSTITUTE OF TECH ATTN L D STRAND MS125 224 JET PROPULSION LAB 4800 OAK GROVE DR PASADENA CA 91109
1	CA INSTITUTE OF TECH ATTN D ELLIOT JET PROPULSION LAB 4800 OAK GROVE DR PASADENA CA 91109
1	MARTIN MARIETTA DEFENSE SYS ATTN DR J MANDZY MAIL DROP 42 220 100 PLASTIC AVE PITTSFIELD MA 01201
1	STATE U OF NY ATTN DR W J SARGEANT DEPT OF ELEC ENGR BONNER HALL RM 312 BUFFALO NY 14260
1	SNL ATTN MR M GRUBELICH DIV 2515 PO BOX 5800 ALBUQUERQUE NM 87185
1	USA BENET LAB ATTN SMCAR CCB R DR S SPOCK WATERVLIET NY 12189
1	US ARMY EUROPEAN RESEARCH OFFICE ATTN DR R REICHENBACH PSC 802 BOX 15 APO AE 09499-1500

NO. OF
COPIES ORGANIZATION

ABERDEEN PROVING GROUND, MD

4 CDR USACSTA
ATTN S WALTON
G RICE
D LACEY
C HERUD
K NEKULA

32 DIR USARL
ATTN AMSRL-WT-P, A HORST
AMSRL-WT-PC,
A FIFER
T KOTLAR
M MILLER
S BUNTE
A COHEN
J HEIMERL
AMSRL-WT-PA,
T MINOR
T COFFEE
M DEL GUERCIO
G KELLER
D KOOKER
F ROBBINS
K WHITE (8 CP)
G WREN
R LIEB
C RUTH
P TRAN
J KNAPTON
A JUHASZ
I STOBIE
G KATULKA
S DRIESEN
AMSRL-WT-PB, E SCHMIDT
AMSRL-WT-PD, B BURNS

NO. OF COPIES	ORGANIZATION
2	RARDE GS2 DIVISION BLDG R31 ATTN DR C WOODLY, DR G COOK FORT HALSTEAD SEVENOAKS KENT TN14 7BP ENGLAND
1	MATERIALS RESESARCH LABORATORY SALISBURY BRANCH ATTN ANNA WILDEGGER GAISSMAIER EXPLOSIVES ORDNANCE DIVISION SALISBURY SOUTH AUSTRALIA 5108
1	LABORATORIO QUIMICO CENTRAL DE ARMAMENTO ATTN CPT JUAN F HERNANDEZ TAMAYO APARTADO 1105 28080 MADRID SPAIN
1	R&D DEPT ATTN DR PIERRE ARCHAMBAULT 5 MONTEE DES ARSENAUX LE GARDEUR QUEBEC CANADA J5Z 2P4

USER EVALUATION SHEET/CHANGE OF ADDRESS

This Laboratory undertakes a continuing effort to improve the quality of the reports it publishes. Your comments/answers to the items/questions below will aid us in our efforts.

1. ARL Report Number ARL-TR-845 Date of Report August 1995

2. Date Report Received _____

3. Does this report satisfy a need? (Comment on purpose, related project, or other area of interest for which the report will be used.) _____

_____

_____

4. Specifically, how is the report being used? (Information source, design data, procedure, source of ideas, etc.)

_____

_____

_____

5. Has the information in this report led to any quantitative savings as far as man-hours or dollars saved, operating costs avoided, or efficiencies achieved, etc? If so, please elaborate. _____

_____

_____

6. General Comments. What do you think should be changed to improve future reports? (Indicate changes to organization, technical content, format, etc.) _____

_____

_____

_____

CURRENT ADDRESS

_____
Organization

_____
Name

_____
Street or P.O. Box No.

_____
City, State, Zip Code

7. If indicating a Change of Address or Address Correction, please provide the Current or Correct address above and the Old or Incorrect address below.

OLD ADDRESS

_____
Organization

_____
Name

_____
Street or P.O. Box No.

_____
City, State, Zip Code

(Remove this sheet, fold as indicated, tape closed, and mail.)
(DO NOT STAPLE)

DEPARTMENT OF THE ARMY

OFFICIAL BUSINESS

NO POSTAGE
NECESSARY
IF MAILED
IN THE
UNITED STATES

BUSINESS REPLY MAIL
FIRST CLASS PERMIT NO 0001,APG,MD

POSTAGE WILL BE PAID BY ADDRESSEE

DIRECTOR
U.S. ARMY RESEARCH LABORATORY
ATTN: AMSRL-WT-PA
ABERDEEN PROVING GROUND, MD 21005-5066